

1 **Competence Inhibition by the XrpA Peptide Encoded Within**
2 **the *comX* Gene of *Streptococcus mutans***

3 Justin Kaspar, Robert C. Shields, and Robert A. Burne*

4

5 Department of Oral Biology, University of Florida, Gainesville, Florida 32610

6

7

8

9 Running title: Antagonism of the ComRS-XIP circuit

10 Keywords: quorum sensing, intercellular signaling, transcription factor, genetic competence,
11 dental caries

12

13 *Corresponding author:

14 Mailing address: Department of Oral Biology, University of Florida, College of Dentistry,

15 P.O. Box 100424, Gainesville, FL 32610.

16 Phone: (352) 273-8850

17 Fax: (352) 273-8829

18 E-mail: rburne@dental.ufl.edu

19

20 **SUMMARY**

21 *Streptococcus mutans* displays complex regulation of natural genetic competence.
22 Competence development in *S. mutans* is controlled by a peptide derived from ComS (XIP);
23 which along with the cytosolic regulator ComR controls the expression of the alternative sigma
24 factor *comX*, the master regulator of competence development. Recently, a gene embedded
25 within the coding region of *comX* was discovered and designated *xrpA* (*comX* regulatory peptide
26 A). XrpA was found to be an antagonist of ComX, but the mechanism was not established. In
27 this study, we reveal through both genomic and proteomic techniques that XrpA is the first
28 describe negative regulator of ComRS systems in streptococci. Transcriptomic and promoter
29 activity assays in the $\Delta xrpA$ strain revealed an up-regulation of genes controlled by both the
30 ComR- and ComX-regulons. An *in vivo* protein crosslinking and *in vitro* fluorescent polarization
31 assays confirmed that the N-terminal region of XrpA were found to be sufficient in inhibiting
32 ComR-XIP complex binding to ECom-box located within the *comX* promoter. This inhibitory
33 activity was sufficient for decreases in P_{comX} activity, transformability and ComX accumulation.
34 XrpA serving as a modulator of ComRS activity ultimately results in changes to subpopulation
35 behaviors and cell fate during competence activation.

36 **ABBREVIATED SUMMARY**

37 *Streptococcus mutans* displays complex regulation of natural genetic competence,
38 highlighted by a novel gene, *xrpA*, embedded within the coding region for the master regulator
39 ComX. We show that XrpA modulates ComRS-dependent activation of *comX* expression,
40 resulting in changes to sub-population behaviors, including cell lysis. XrpA is the first described
41 inhibitor of a ComRS system and, because it is unique to *S. mutans* it may be targetable to
42 prevent diseases caused by this pathogen.

43 INTRODUCTION

44 Bacterial biofilm communities coordinate behaviors in response to environmental stimuli
45 through the use of chemical mediators that accumulate extracellularly to activate transcription of
46 specific genes when a critical concentration is achieved, in a process termed quorum sensing
47 (Fuqua *et al.*, 1994). In Gram-negative bacteria, diffusible acylated homoserine lactones are the
48 principal chemical mediator that act as a proxy for cell density (Papenfort and Bassler, 2016),
49 whereas small hydrophobic peptides fulfill a similar role in Gram-positive bacteria (Håvarstein *et al.*
50 *et al.*, 1995). More recently, quorum sensing and gene products involved in intercellular signaling
51 have been highlighted as an area of interest for therapeutic intervention in some bacterial
52 infections, because quorum sensing often controls the transcription of genes that contribute to
53 virulence (Greenberg, 2003).

54 Genetic competence, a transient physiological state in which bacteria produce the gene
55 products necessary for uptake of DNA from their environment was one of the first described and
56 studied quorum sensing pathways (Tomasz, 1965). Decades later, genetic competence is still a
57 valuable model system in molecular microbiology to unravel the complexities of signal
58 perception, signal transduction and sub-population behaviors, and is of relevance to newer
59 areas of research that include sociomicrobiology, interspecies antagonism and cooperativity,
60 and microbial biogeography (Whiteley *et al.*, 2017). Genetic competence has been extensively
61 studied in the genus *Streptococcus*, including *Streptococcus pneumoniae* (Hui *et al.*, 1995;
62 Straume *et al.*, 2015), *Streptococcus thermophilus* (Fontaine *et al.*, 2009; Gardan *et al.*, 2013),
63 *Streptococcus pyogenes* (Mashburn-Warren *et al.*, 2012; Wilkening *et al.*, 2015) and
64 *Streptococcus mutans* (Li *et al.*, 2001; Son *et al.*, 2012). Interestingly, streptococci harbor two
65 distinct peptide signaling systems that activate genetic competence: the Mitis and Anginosus
66 groups utilize an extracellular signaling system composed of a signaling peptide termed CSP
67 (competence stimulating peptide) and a two-component signal transduction system encoded by
68 *comDE*. In contrast, the Bovis, Salivarius and Pyogenic streptococci employ an intercellular

69 signaling system that consists of the signal peptide XIP (*comX/sigX* inducing peptide) derived
70 from the ComS precursor, and a cytosolic Rgg-like regulator designated as ComR (Håvarstein,
71 2010). While these two signal systems diverge substantially in their distribution among species
72 and how the systems perceive and transduce their signals, stimulation of either pathway with
73 the cognate peptide results in the activation of transcription of an alternative sigma factor
74 termed ComX or SigX. ComX controls the transition into the competent state by activating the
75 expression of a regulon encoding gene products necessary for DNA uptake and processing.

76 The Mutans group of streptococci, including the human caries pathogen *S. mutans*, are
77 unique in that most strains encode an apparently functional ComCDE as well as ComRS
78 pathways. Further, either signal peptide (CSP or XIP) can trigger up-regulation of *comX*,
79 although different conditions, including pH, redox and growth phase, influence how effectively
80 each pathway is able to function (Hagen and Son, 2017). Addition of synthetic CSP (sCSP) to
81 growing cultures of *S. mutans* in a peptide-rich medium, such as BHI, results in activation of
82 transcription of genes for the biogenesis of bacteriocins via direct binding of phosphorylated
83 ComE to a conserved sequence in the promoter regions of these genes and operons.
84 Consistent with this observation, the ComCDE system of *S. mutans* appears to have evolved
85 from a common ancestor of the BIpCRH system of *S. pneumoniae*, which does not regulate
86 competence but does induce bacteriocins in the pneumococcus and some related organisms
87 (Johnston *et al.*, 2014). Transcription of *comX* can also be induced by CSP, but this generally
88 occurs in only a subset of organisms in a population, it does not involve direct binding of ComE
89 to the *comX* promoter, and the underlying mechanism for CSP-dependent activation of *comX* is
90 not well-understood (Kreth *et al.*, 2007; Hung *et al.*, 2011). The proximal regulator for direct
91 activation of competence is ComRS. When synthetic XIP (sXIP) is added to a peptide-free,
92 chemically defined medium, such as FMC or CDM, it is imported into the cytosol by the
93 oligopeptide permease OppA and forms a complex with ComR to activate *comX* transcription in
94 the entire bacterial population (Mashburn-Warren *et al.*, 2010; Son *et al.*, 2012). The XIP-ComR

95 complex can also activate the gene for the precursor of XIP, *comS*, creating a positive feedback
96 loop for amplification of the competence activation signal (Fontaine *et al.*, 2013). XIP has been
97 detected in culture supernates, supporting the hypothesis that XIP is a diffusible intercellular
98 signal (Desai *et al.*, 2012; Khan *et al.*, 2012; Wenderska *et al.*, 2012), although the mechanism
99 by which XIP is released into the environment can involve active transport (Chang and Federle,
100 2016) or cell lysis (Kaspar *et al.*, 2017), depending on the species of bacteria. Recently, it was
101 confirmed experimentally that XIP is able to act as a diffusible intercellular communication
102 molecule and that signaling can occur within biofilm populations (Shields and Burne, 2016;
103 Kaspar *et al.*, 2017).

104 While substantial progress has been made dissecting the mechanisms leading to *com*
105 gene activation, very little is known about regulation of the system after *comX* is induced and
106 late competence gene expression is active. In *S. pneumoniae*, shut-off of the ComCDE system
107 is regulated at multiple levels, including competition between phosphorylated and un-
108 phosphorylated ComE for binding sites, direct inhibition of activated ComE by the late
109 competence gene-encoded protein DprA, and by inhibition of ComX activity by an unknown
110 factor (Martin *et al.*, 2013; Mirouze *et al.*, 2013; Weng *et al.*, 2013). In streptococci that harbor
111 ComRS systems, the factors that regulate the Com circuit after transcriptional activation have
112 not been characterized in significant detail. It has been postulated that a “*comZ* gene”, under the
113 control of ComX, exists that encodes a product that acts on the ComR-XIP complex to create a
114 feedback inhibition loop (Boutry *et al.*, 2013; Haustenne *et al.*, 2015). Recently, we described a
115 novel protein encoded within *comX* gene in an alternative (+1) reading frame that we
116 designated as XrpA (*comX* regulatory protein/peptide A) (Kaspar *et al.*, 2015). We described
117 XrpA as a novel antagonist of *comX* as loss of XrpA, either by mutating the start codon or by
118 introducing premature stop codons, led to an increase in transformation efficiency and
119 accumulation of the ComX protein, whereas overexpression of *xrpA* resulted in decreased
120 transformability and lower levels of ComX. However, the mechanism by which XrpA exerted its

121 effects was not determined. In this study, we present genetic evidence through transcriptome
122 profiling and biochemical evidence of protein-protein interactions that demonstrate that XrpA
123 affects competence development in *S. mutans* by interacting with and inhibiting ComR activity,
124 thus describing the first negative regulator of competence signaling that acts on the ComRS
125 circuit.
126

127 RESULTS

128 *Transcriptome profiling of an XrpA-deficient strain*

129 In our initial characterization of *xrpA*, we highlighted the unusual transcriptional
130 characteristics of *xrpA* and the profound influence of XrpA on the dramatically different genetic
131 competence phenotypes displayed by strains with polar and non-polar mutations in the *rcrR*
132 gene of the *rcrRPQ* operon, designated $\Delta rcrR$ -P and $\Delta rcrR$ -NP, respectively. Inactivation of
133 *xrpA* in a way that did not alter the primary sequence of ComX could convert the non-
134 transformable $\Delta rcrR$ -NP strain into the hyper-transformable state that was observed for the
135 $\Delta rcrR$ -P strain, with concomitant restoration of ComX production (Kaspar *et al.*, 2015). However,
136 the *rcrR* mutants displayed extreme and unusual phenotypes, so questions remain as to how
137 *xrpA* expression is regulated and what role XrpA plays in a wild-type *S. mutans* genetic
138 background. To begin to answer these questions, we first wanted to compare the
139 transcriptomes of a $\Delta xrpA$ strain with that of the *S. mutans* wild-type strain, UA159. For these
140 studies and those conducted henceforth, the $\Delta xrpA$ used contains a single base change at the
141 162nd nucleotide of *comX* (*comX*::T162C), which mutates the *xrpA* start codon (ATG→ACG) and
142 leaves the *comX* protein coding sequence unchanged (Kaspar *et al.*, 2015).

143 Comparison of the transcriptome by RNA-Seq of the wild-type with the mutant lacking
144 XrpA when cells were grown in the chemically defined medium FMC to mid-exponential phase
145 revealed 56 differentially expressed genes, with 34 upregulated in $\Delta xrpA$ and 22 downregulated
146 **(Figure 1A)**. Many of the upregulated genes were competence-related genes, including *comX*
147 and genes that are a part of the ComX regulon of *S. mutans* (Khan *et al.*, 2016) **(Table S2)**.
148 Since loss of *xrpA* caused upregulation of competence genes, we also analyzed the
149 transcriptome of UA159 treated with 2 μ M sXIP to induce competence, with UA159 treated with
150 vehicle (DMSO) as a control. Cells treated with sXIP had 137 genes differentially expressed
151 compared to the control **(Figure 1B; Table S3)**. Several of the same genes that were the most

152 strongly upregulated in $\Delta xrpA$, including the *comF* and *comY* operons, *drpA* and *lytF*, were also
153 the highest upregulated genes in the sXIP-treated cells. Interestingly, those genes that were
154 downregulated in the $\Delta xrpA$ strain differed from those downregulated by sXIP addition to
155 UA159. All of the downregulated genes in the $\Delta xrpA$ mutant were located on the TnSMu1
156 genomic island that encodes predicted transposases, integrases, transporter(s) and
157 hypothetical proteins (Waterhouse *et al.*, 2007). This genomic island was recently found to be
158 differentially expressed in *clpP* and *cidB* mutants, providing additional evidence for a link
159 between XrpA and stress responses (Chattoraj *et al.*, 2010; Kaspar *et al.*, 2015; Ahn and Rice,
160 2016).

161 Meanwhile, the upregulation of the ComX regulon in the $\Delta xrpA$ mutant could not be
162 explained by increases in expression of annotated early competence genes. However, when we
163 examined the region encoding *comS*, which is encoded in the intergenic region of SMU.61 and
164 SMU.63c in current database annotations, we found an elevated number of reads for *comS* in
165 the $\Delta xrpA$ strain compared to UA159 (**Figure 1C**). When one considers that both *comS* and
166 *comX* are upregulated in the XrpA-deficient strain, a clearer picture emerges that XrpA most
167 likely exerts its influence over competence development by influencing the efficiency of ComR-
168 dependent activation of the *comX* and *comS* promoters, *PcomX* and *PcomS*.

169

170 *XrpA alters comX and comS promoter activity*

171 To determine if XrpA affects the ComR-XIP activated promoters, *PcomX* and *PcomS*, we
172 incorporated the *xrpA* start codon mutation *comX*::T162C into strains carrying GFP
173 transcriptional fusions to each promoter. Similarly, we transformed an *xrpA*-overexpressing
174 strain (184XrpA) into the GFP reporter gene fusion strains to see if increasing the amount of
175 XrpA produced would yield gene expression patterns that were opposite of those caused by
176 loss of *xrpA*. Cells were grown in chemically defined CDM, which allows for self-activation of the

177 ComRS system. Indeed, loss of *xrpA* resulted in both earlier and higher level expression of
178 *PcomX* and *PcomS* reporters, compared to what was observed in the wild-type genetic
179 background. Conversely, overexpression of *xrpA* from the strong, constitutive promoter on
180 pIB184 caused a decrease in GFP production from the *comX* and *comS* promoters (**Figure 2**).
181 Collectively, these results validate the RNA-Seq data and provide support for the hypothesis
182 that XrpA negatively affects the activation of gene expression by ComR.

183

184 *XrpA influences subpopulation responses to competence signals*

185 Stimulation of genetic competence in a peptide-rich medium, such as brain-heart
186 infusion (BHI), by CSP results in a bimodal response where only a sub-population of cells
187 activate *PcomX* (Son *et al.*, 2012). We reasoned that XrpA might influence the proportion of
188 cells that responded to sCSP in BHI. We utilized both the wild-type and $\Delta xrpA$ mutant carrying
189 *PcomX* transcriptional reporter gene fusions and analyzed subpopulation behaviors using flow
190 cytometry three hours after sCSP addition to planktonic cultures. The percentage of cells that
191 were GFP-positive was more than 20% greater in the $\Delta xrpA$ background with addition of 100 nM
192 sCSP (39.7 ± 2.2 versus 61.5 ± 1.8) (**Figure 3A**) or 1000 nM sCSP (48.7 ± 1.4 compared to
193 73.9 ± 2.3) (**Figure 3B**). Further, mean GFP fluorescence intensity was increased in the $\Delta xrpA$
194 background.

195 Stimulation of the competence cascade by XIP in nanomolar concentrations of wild-type
196 *S. mutans* growing in a peptide-free medium results in a unimodal population response, but
197 addition of sXIP to cultures of *S. mutans* at concentrations higher than 1 μ M can trigger cell
198 death in a significant fraction of the population (Wenderska *et al.*, 2012). To determine if XrpA
199 could influence XIP-mediated killing in cells treated with higher concentrations of sXIP, we
200 followed a protocol similar to the CSP experiments, but stained the cells with propidium iodide
201 (PI) to measure membrane integrity prior to analysis by flow cytometry. No changes were seen

202 in the proportions of the population that were PI-positive between the wild-type and $\Delta xrpA$
203 background, but a clear increase in the mean GFP intensity was observed when *xrpA* was
204 mutated, similar to what was seen with CSP (**Figure 3C**). However, when the *comS* gene was
205 removed to eliminate the positive feedback loop in the XIP signaling pathway, a distinct increase
206 in the proportion of PI-positive cells was seen in the $\Delta xrpA$ mutant population, compared to
207 behaviors in the wild-type genetic background (36.8 ± 0.7 versus 47.2 ± 0.9) (**Figure 3D**).
208 Measurements of eDNA release from overnight cultures were used to confirm the finding that
209 strains that were activated for competence, but that lack *xrpA*, were more lytic than their wild-
210 type counterparts (**Figure 3E**). This lytic behavior could also be measured in a biofilm model,
211 where the absence of XrpA correlated with decreased biofilm formation after 48 h, compared to
212 increased biofilm formation in the non-competent $\Delta comR$ or $\Delta comX$ mutant strains (**Figure 3F**).
213 Taken together, these data highlight that XrpA can influence subpopulation behaviors both in
214 terms of competence activation in environments where peptides are present, and influence lytic
215 behaviors associated with activation of the competence by high, albeit physiologically relevant,
216 concentrations of signal peptide, with the enhanced cell death most likely being associated with
217 more robust activation of *PcomX*.

218

219 *Addition of XrpA can inhibit competence development*

220 As data from transcriptome profiling and transcriptional reporter experiments support a
221 role for XrpA in interference with the ComRS pathway, we wanted to test whether direct addition
222 of XrpA could inhibit competence development. We tried various strategies to produce a full-
223 length recombinant XrpA in *Escherichia coli*, however we were unsuccessful, possibly due to
224 the combination of its hydrophobicity and having 7 cysteines distributed across the protein. As a
225 substitute, we settled on synthesizing four different peptide fragments that span the entirety of
226 the 69-aa XrpA protein (**Figure 4A**). We first tested the ability of the peptides to interfere with

227 activation of the *PcomX* transcriptional reporter in cells growing in CDM. Of the four peptides
228 tested, only XrpA-1 containing aa 5-20 of the N-terminal region of the protein caused a marked
229 decreased in *PcomX* activity, compared to when only vehicle was added (**Figure 4B**).
230 Interestingly, a higher final OD₆₀₀ was also recorded for cultures exposed to XrpA-1, compared
231 to when either vehicle or any of the other three peptides were tested. To confirm that this effect
232 was specific for XrpA-1, a scrambled peptide (XrpA-S1; same aa composition, different
233 sequence) was synthesized and tested (**Figure 4A**). While some residual inhibitory activity was
234 evident with the scrambled peptide, compared with control and other peptides, the effects of the
235 scrambled peptide was much less pronounced than XrpA-1 (**Figure 4C**). The inhibitory effect of
236 the XrpA-1 peptide was also found to be dose-dependent in this experimental setup (**Figure**
237 **4D**). A similar profile for XrpA-1 was seen using the ComR-XIP activated *PcomS::gfp*
238 transcriptional fusion strain (data not shown). Together, these results confirm that selected XrpA
239 fragments can inhibit ComRS-dependent activation of *comX* when provided exogenously to
240 cells growing in a chemically defined medium. It is important to note that we presently have no
241 data to support that XrpA peptides are excreted or follow a similar lifecycle as XIP. We contend
242 that observing a response by providing the peptides exogenously was a fortuitous occurrence
243 and future studies will be needed to understand the mechanism for the effect.

244 An explanation for the higher OD₆₀₀ values when XrpA-1 was added to the growing
245 cultures may be related to reduced cell lysis from decreased competence activation. eDNA
246 release was measured as described for Figure 3 and we found significantly less eDNA
247 accumulation in culture supernates from overnight cultures grown in the presence of XrpA-1, but
248 not with the other XrpA peptides, compared to DMSO-treated controls. (**Figure 5A**). We also
249 tested several other competence-related phenotypes with the synthetic XrpA peptides. In terms
250 of transformation efficiency, a significant -1.22 ± 0.05 -Log₁₀ fold decrease was observed when
251 XrpA-1 was present, compared to the DMSO only control, and -0.23 ± 0.07 and -0.08 ± 0.19 -
252 Log₁₀-fold decreases were observed when XrpA-2 and XrpA-3 were present, respectively

253 **(Figure 5B)**. In terms of ComX accumulation, ComX protein was not observed by western
254 blotting in cells treated with XrpA-1 **(Figure 5C)**. It did not appear as if ComR levels were
255 impacted by addition of any of the peptides, suggesting that XrpA does not influence ComRS
256 activity by altering ComR stability. In all, these results support the gene fusion assays and show
257 that XrpA addition to growing cultures has a significant impact on competence development and
258 lysis-related phenotypes when provided exogenously to *S. mutans*.

259

260 *In vitro interactions of XrpA and ComR*

261 We hypothesized that XrpA inhibits competence development through direct interaction
262 with ComR, affecting ComR DNA binding activity and leading to reduced *P_{comX}* activation. To
263 confirm this hypothesis, we utilized a fluorescence polarization (FP) assay where we could
264 monitor the binding of the ComR-XIP complex to the promoter region of *comX in vitro* using
265 purified ComR protein and a 5' Bodipy-labeled, self-annealing stem-loop DNA probe that
266 encompassed the ECom-box to which ComR-XIP binds for transcriptional activation (Mashburn-
267 Warren *et al.*, 2010; Fontaine *et al.*, 2013). Strong, direct binding of ComR-XIP was observed to
268 the probe in the absence of any of the XrpA peptides, with a calculated K_d of 153 ± 10 nM
269 **(Figure 6A, Table 2)**. However, when XrpA-1 was added to the reaction, the K_d increased to
270 651 ± 99 nM. Surprisingly, XrpA-2, which had no observable effects on the phenotypes
271 examined above, also displayed inhibitory effects, while inclusion of XrpA-3 or XrpA-4 did not
272 substantially alter the calculated K_d values **(Table 2)**. Two different scrambled peptides as
273 detailed in Figure 4A, containing the same aa composition as their respective counterpart but
274 different sequence, were tested in combination with XrpA-1 and XrpA-2 to verify the specificity
275 of the effect. Similar to the transcriptional reporter assays, XrpA-S1 showed some alleviation of
276 inhibitory properties **(Figure 6B)**, whereas inclusion of the XrpA-2 scrambled peptide yielded a
277 ComR-XIP DNA binding affinity similar to the control **(Figure 6C, Table 2)**. Taken together,
278 these experiments verify that XrpA interacts directly with ComR, with the outcome being that

279 this interaction antagonizes promoter binding and ultimately gene expression by the ComR-XIP
280 complex and competence development.

281

282 *The N-terminal region of XrpA directly interacts with ComR*

283 Using our four synthesized peptide fragments of XrpA, it appeared that the N-terminal
284 region of XrpA was the domain responsible for the inhibitory activity. To confirm that the *in vitro*
285 protein-protein interaction data accurately represented *in vivo* activity, we adapted a Strep-
286 protein interaction (SPINE) protocol (Herzberg *et al.*, 2007) that allows for crosslinking of
287 proteins *in vivo*, followed by affinity purification of target protein complexes and identification of
288 interacting partners using mass spectrometry (MS). For this experiment, we chose ComR as the
289 bait by incorporating a C-terminal Strep-tag[®] in front of the stop codon. The construct was also
290 engineered in such a way as to introduce 9 amino acids to serve as a flexible linker sequence to
291 minimize the potential for disrupting the native conformation of ComR; interaction of small
292 hydrophobic peptides by Rgg-like regulators occurs with the C-terminal domain of the proteins
293 (Talagas *et al.*, 2016). Cultures (500 ml) of a strain carrying the Strep-tagged ComR expressed
294 from the strong constitutive promoter on pIB184, and a vector-only control strain, were grown in
295 CDM to mid-exponential phase ($OD_{600} = 0.6$), at which point either 2 μ M sXIP or an equivalent
296 volume of 0.1% DMSO control were added. After growth for an additional hour ($OD_{600} = 0.8$), the
297 homobifunctional *N*-hydroxysuccinimide ester (DSP) cross-linking agent that is primary amine-
298 reactive and contains a thiol-cleavable bridge was added to the cells for 45 minutes at 37°C,
299 cells were harvested, and clarified whole cell lysate were passed over a Strep-Tactin[®] resin for
300 isolation of the targeted complex, as detailed in the methods section (**Supplemental Figure 1**).

301 In our initial experiments, purified protein complexes were subjected to SDS-PAGE,
302 followed by silver staining (**Supplemental Figure 2**). Five bands of interest that appeared in the
303 Strep-tagged ComR sample, but not in the vector control sample, were excised from the gel and
304 identified by LC-MS/MS after trypsin digestion (**Supplemental Table 5**). Peptide fragments

305 were identified that were derived from the transcriptional regulator SgaR (SMU.289) and a
306 putative single-stranded DNA binding protein Ssb2 encoded by SMU.1967, as well as peptides
307 derived from XrpA. In a second experiment, the purified protein complexes were subjected to
308 two-dimensional differential gel electrophoresis (2D DIGE) (**Figure 7A, Supplemental Figure**
309 **3**). A total of 58 spots of interest were selected and a protein expression ratio (PER) was
310 calculated between triplicate samples (**Supplemental Table 4**). Spots chosen for identification
311 were required to have a PER >1.5 compared to the vector-only control sample. The selected
312 spots, 28 in total, were then excised from the gel, digested by trypsin, peptide sequences
313 identified by LC-MS/MS and then compared to a list of predicted masses for all *S. mutans*
314 proteins. While several *S. mutans* proteins were identified with high confidence (**Supplemental**
315 **Table 5**), peptides derived from XrpA were identified from the 2D DIGE and the fragments
316 detected originated exclusively from the N-terminus of XrpA (aa 1-38), with the fragment
317 MFCVSKK being the peptide that was most frequently observed. Notably, one of the most
318 frequently identified peptide fragments of XrpA observed in the SPINE experiment was not part
319 of the sequence of XrpA-1, so we speculated that using larger peptides might elicit a stronger
320 inhibitory effect. Peptides N1 and N2 were synthesized that included aa 1-18 and aa 18-38,
321 respectively, encompassing all identified XrpA fragments (**Figure 7B**). Indeed, XrpA-N1
322 substantially decreased *PcomX* activity, similar to XrpA-1, whereas addition of XrpA-N2 had an
323 intermediate effect compared to the DMSO control (**Figure 7C**). Similar to the growth profiles of
324 the transcriptional reporter strains seen in Figure 4B, XrpA-N1 also displayed better growth,
325 compared to when XrpA-N2 or vehicle was added. These results were mirrored in fluorescent
326 polarization experiments with recombinant ComR and the *PcomX* probe (**Figure 7D**). In all,
327 these experiments implicate the N-terminal region of XrpA in interactions with ComR.

328

329 *Binding of XrpA to ComR is not dependent on the comX promoter*

330 While the results described thus far suggest that N-terminal fragments of XrpA are
331 sufficient to diminish the ability of ComR to bind DNA, the effect could be exerted in multiple
332 ways. For example, (1) XrpA could interact directly with the ComR-XIP oligomer(s) to decrease
333 the affinity of the complex for DNA, (2) XrpA could compete with XIP for the SHP (XIP) binding
334 site, or (3) XrpA may inhibit ComR-dependent activation of gene expression by preventing
335 ComR-XIP from forming higher-order oligomeric complexes; the ComR-XIP complex forms
336 dimers upon XIP binding (Fontaine *et al.*, 2013). To further explore how XrpA influences ComR
337 behavior, we synthesized a fluorescein isothiocyanate (FITC)-labeled XrpA-N1 peptide and
338 monitored its direct binding to ComR by FP in the absence of the *PcomX* DNA probe. We tested
339 the specificity of the FITC-labeled XrpA-N1 peptide probe interaction with ComR by doing
340 fluorescent polarization experiments with two other *S. mutans* purified proteins that do not
341 participate directly in the regulation of competence, CcpA (Abranches *et al.*, 2008) and SppA
342 (SMU.508; Zeng, personal communication), and neither showed any ability to interact with
343 fluorescent XrpA-N1 (**Figure 8A**). We also conducted a cold competition FP assay and found
344 poorer binding for our peptide probe to ComR as increasing concentrations of unlabeled XrpA-
345 N1 peptide were added (**Figure 8B**). In terms of experiments with ComR, fluorescence
346 polarization in the presence of XrpA-N1 was increased regardless of whether sXIP was present
347 or absent (**Figure 8C**), indicating that XrpA may interact directly with ComR and that this
348 interaction can occur even if XIP does not occupy the SHP-binding pocket. Finally, addition of
349 increasing concentrations of sXIP had no effect on fluorescent XrpA-N1 affinity for ComR
350 (**Figure 8D**), suggesting that XrpA and sXIP do not compete for the SHP (XIP) binding site.
351 Collectively, these experiments verify that XrpA interacts directly with ComR independent of
352 both ComR-regulated promoters (such as *PcomX*) as well as XIP, favoring a model where XrpA
353 inhibits ComRS activity through disruption of ComR-XIP dimer formation, leading to measurable
354 decreases in *PcomX* activity, in ComX production and ultimately in a muted activation of
355 competence (**Figure 9**).

356 DISCUSSION

357 The study of bacterial cell-cell communication has provided valuable insights into
358 bacterial processes that are critical for growth, essential for the activities of complex microbial
359 ecosystems, and impactful of human health and diseases. These communication pathways
360 have served as tractable model systems to dissect the intricacies of specialized secretory
361 systems for signal molecules and bacteriocins, the mechanisms for signal transduction through
362 two-component systems and cytosolic transcriptional regulators, the hierarchical control of
363 regulons, and how multiple sensory inputs are integrated into key physiological outcomes and
364 manifestation of virulence. As research has continued with these systems, the apparently
365 straightforward paradigms once described for control of quorum sensing and intercellular
366 communication have been assimilated into increasingly complex and diverse models for cellular
367 reprogramming. Examples of such complexity can be found with negative feedback associated
368 with the late competence gene *dprA* of *Streptococcus pneumoniae* (Weng *et al.*, 2013),
369 identification of the novel protein Kre that controls the bimodal regulation of ComK in *Bacillus*
370 *subtilis* (Gamba *et al.*, 2015), and the recent discovery of a short, leaderless, intercellular
371 peptide signal in Group A *Streptococcus* (Do *et al.*, 2017) that regulates protease expression.
372 Similar advances in understanding of regulatory systems have been realized using *S. mutans*
373 as a model organism (Lemos *et al.*, 2013). One important characteristic that distinguishes *S.*
374 *mutans* from other streptococci is that it encodes the ComRS signaling systems and integrates
375 the ComCDE bacteriocin production pathway with competence through at least two different
376 signal peptides XIP and CSP, respectively. Here we demonstrate additional complexities in the
377 competence pathway of *S. mutans*, which is intimately intertwined with stress tolerance (Kaspar
378 *et al.*, 2016), by providing experimental evidence that a novel negative feedback system
379 involving the unusual XrpA peptide is a regulator of the ComRS pathway and, consequently, of
380 activation of late competence genes and lytic behaviors.

381 Using genetic and biochemical approaches, we confirmed that XrpA serves as a
382 negative regulator of competence development in *S. mutans* by inhibiting activation of the
383 targets of the ComR-XIP complex, apparently through a direct interaction with ComR that can
384 be demonstrated *in vivo* by cross-linking and *in vitro* using purified constituents. We first
385 described XrpA as an antagonist of ComX (Kaspar *et al.*, 2015) that, based on its unusual
386 genomic location within the *comX* gene and the inverse relationship of *xrpA*-specific mRNA
387 abundance to the full-length *comX* transcript and ComX protein levels, might function as an anti-
388 sigma factor, as opposed to acting on early competence genes (ComDE or ComRS systems).
389 Instead, using transcriptome profiling and transcriptional reporter assays a picture began to
390 emerge that XrpA influenced ComRS-dependent activation of the *comX* promoter. XrpA
391 functioning as an autogenous negative regulator of its own expression by blocking ComR-
392 dependent activation of *comX* may provide the cells with an opportunity to fine-tune ComS and
393 ComX production, particularly in response to environmental inputs, such as redox. A similar type
394 of regulation has been described for the *E. coli* RNA polymerase-binding protein DksA, which
395 along with the co-factor (p)ppGpp promotes a negative feedback loop on the *dksA* promoter to
396 keep DksA protein levels constant in different environmental conditions (Chandrangsu *et al.*,
397 2011). Not only is it intriguing in evolutionary terms that the XrpA negative feedback system
398 evolved within the *comX* coding region, but also there are potentially important physiological
399 ramifications of the existence of this regulatory circuit. The exact mechanism by which the *xrpA*
400 mRNA is translated has not been established, but we presently favor a model by which
401 ribosomal slippage occurs during *comX* translation at or near the *xrpA* start codon, allowing for
402 production of XrpA, with the efficiency of translational initiation at the *xrpA* start codon and the
403 stability of the 5' region of the *comX* mRNA being factors that govern the ratio of ComX to XrpA.
404 Confirmation of such a model is the subject of ongoing research. Nevertheless, if we accept the
405 premise that *xrpA* translation is not as efficient as that of *comX* when the *comX* promoter is
406 activated, then it can be envisioned that the negative feedback loop created by XrpA acting on

407 ComR modulates transcriptional initiation at the *comX* promoter; with the feedback loop
408 contributing to fine tuning ComX levels in response to cellular physiology and environment
409 and/or serving as a primary pathway to turn off the competence circuit. The former would be
410 consistent with the observation that signal perception, induction of *comX* and progression to the
411 competent state are all exquisitely sensitive to key environmental inputs that include pH (Guo *et*
412 *al.*, 2014; Son *et al.*, 2015), oxidative stressors (De Furio *et al.*, 2017) and carbohydrate source
413 and availability (Moye *et al.*, 2016). The latter model would be consistent with the fact that, while
414 the MecA-Clp pathway can serve as a mechanism to shut off competence through degradation
415 of ComX, the cells also need a way to shut down the ComRS circuit so as not to produce
416 nascent ComX during competence while committing to turning off the competence regulon.

417 Our model for XrpA acting at the level of ComR-dependent activation of *comS* and *comX*
418 is supported by the transcriptional reporter data in which overexpression of *xrpA* lead to
419 decreased *PcomX* activity (Figure 2). Recently it was suggested that an antagonist termed
420 “ComZ” must be present within ComRS-positive streptococci that can shut down ComRS
421 activity in a similar manner to DprA of the ComDE systems (Mirouze *et al.*, 2013; Haustenne *et*
422 *al.*, 2015). We do not suspect that XrpA is the aforementioned ComZ, as the loss of *xrpA* only
423 exhibits stronger activation of ComRS-dependent promoters, but does not increase the duration
424 of activation, as is evident in Figure 2. Studies into ComX stability over the course of
425 competence activation revealed that ComX protein accumulates faster at early time points after
426 induction with signal peptides (10-30 minutes) in an *xrpA*-negative strain, consistent with the
427 data on promoter activity, but ComX protein dissipates at a similar rate in the presence or
428 absence of *xrpA* (data not shown). Thus, we conclude that XrpA modulates the strength of
429 ComRS signaling, but other factors must be present, possibly working in concert with XrpA, to
430 shut off competence in *S. mutans*, further highlighting the complexity of these systems. There is
431 potential for other protein candidates identified in our SPINE experiment, such as *ssb2*, fulfill
432 this role; an area that remains to be investigated.

433 In *S. mutans*, competence activation has been linked to cell lysis in a process similar to
434 the fratricide that was first described for *S. pneumoniae*. Fratricide appears to be essential for
435 efficient gene transfer between bacteria in biofilm communities and to be mediated in *S. mutans*
436 through the activities of encoded cell wall hydrolases that are a part of the ComX regulon (Wei
437 and Håvarstein, 2012; Khan *et al.*, 2016), and possibly by intracellular bacteriocins (Perry *et al.*,
438 2009). As seen in Figure 3, the inhibition of ComRS activity by XrpA has the ability to change
439 the proportion of cells exhibiting responses to signal inputs in a population, both in terms of
440 competence activation in complex medium and cell lysis, as measured by propidium iodide
441 staining of XIP-treated cultures and production of eDNA, which in *S. mutans* is heavily
442 dependent on cell lysis (Liao *et al.*, 2014). We propose a model (**Figure 9**) in which *xrpA*
443 influences the decision pathway by which cells choose between a) viability and potential to
444 uptake DNA as a result of competence activation or b) fratricide and cell death, the latter
445 providing a source of genetic material and eDNA for incorporation into the extracellular matrix
446 during biofilm formation (Liao *et al.*, 2014). We posit that this decision network relies on the
447 strength and duration of *PcomX* activation, although we cannot yet rule out the post-
448 transcriptional regulatory factors (RNA binding proteins, RNAses, or riboswitching) govern the
449 ratio of XrpA to ComX. Notwithstanding, when XrpA accumulates and/or is active, the strength
450 of ComRS activation is moderated, providing an even balance between cell viability and cell
451 death. In the absence of XrpA, ComRS-dependent activation causes ComX over-accumulation,
452 which favors lytic behavior, which can be observed in Figure 3 and is supported by the fact that
453 higher concentrations of exogenously supplied XIP induce cell death (Wenderska *et al.*, 2012).
454 Previously, we reported that overexpression of *xrpA* results in a growth defect in the presence of
455 oxygen, linking *xrpA* expression and production to oxidative stress tolerance (Kaspar *et al.*,
456 2015). One aspect not studied here is how *xrpA* might sense an oxidative environment and
457 integrate that response into competence activation through modulation of ComRS activity. The
458 C-terminal portion of XrpA, which does not appear to interact with ComR, is very hydrophobic

459 and may be membrane-associate (Kaspar *et al.*, 2015). Additionally, XrpA is unusual in that it
460 contains seven cysteine residues distributed fairly evenly across the protein that could
461 participate in disulfide bond formation, between XrpA proteins/peptides to influence XrpA
462 availability or to form covalent interactions with binding partners. ComR contains three cysteine
463 residues distributed evenly over its length, which could allow for covalent coupling to XrpA or
464 sub-fragments of XrpA. It is our working hypothesis that XrpA integrates the oxidative state of
465 the environment into fine-tuning the strength of the ComRS signal, tempering activation in one
466 condition over the other. In the case of early biofilm formation, oxygen is readily available and
467 could be sensed by environmental inputs such as XrpA, leading to its inactivation. In this
468 scenario, high ComRS activation and ComX accumulation could shift a larger population of the
469 cells into a lytic mode during competence activation, releasing eDNA to facilitate the formation
470 of a protective extracellular matrix, thereby conveying increased fitness or persistence of *S.*
471 *mutans* over other health-associated commensal streptococci. As oxygen levels and redox
472 potential decrease with biofilm maturation, the need for strong competence activation could be
473 diminished, shifting the cells into a more stable growth mode with a smaller proportion of cells
474 undergoing lysis. It is noteworthy also that bacteriocins are among the most highly up-regulated
475 genes when *S. mutans* is growing in air, compared with the transcriptome of anaerobically
476 growing cells (Ahn *et al.*, 2007). We are currently exploring these ideas and how the
477 competence regulon is integrated with biofilm development and its role in competition with
478 commensal streptococci. It is critical to note that ComX and XrpA are highly conserved in all
479 sequenced clinical isolates of *S. mutans* (Kaspar *et al.*, 2015), suggesting evolutionary pressure
480 to keep these pathways intact. Our working hypothesis is this evolutionary pressure arises from
481 the need to compete with commensal streptococci that can antagonize the growth of *S. mutans*
482 through a variety of mechanisms (Bowen *et al.*, 2017).

483 We have previously noted that *xrpA* appears to be unique to *S. mutans* (Kaspar *et al.*,
484 2015). Indeed, a tblastn search for identification of ORFs with similar sequences bacteria

485 showed that only *Streptococcus troglodytae*, a recently sequenced oral isolate from
486 chimpanzees that is most closely related to *S. mutans* (Okamoto *et al.*, 2013), contains an intact
487 *xrpA* coding sequence embedded within the *comX* coding region. *Streptococcus dysgalactiae*
488 subsp. *equisimilis* (SDSE) also contains a similar *xrpA* coding sequence, but the *xrpA* protein
489 coding sequence is disrupted by premature stop codons in the sequenced isolate of this
490 *Streptococcus*. Thus, it appears that only *S. mutans* and extremely closely related organisms
491 are the only ComRS-containing streptococci that encode an XrpA-like inhibitor; there is no
492 evidence that XrpA is present in *S. rattus*, *S. sobrinus*, *S. cricetus*, *S. downeii* or other mutans
493 streptococci. We cannot, however, exclude that there are proteins or peptides in ComRS-
494 containing streptococci that play a role that is similar or identical to that of XrpA in *S. mutans*.
495 The unique nature of XrpA in *S. mutans* is also notable in the context that the *S. mutans* ComR
496 has strict recognition for its cognate XIP peptide (Shanker *et al.*, 2016), whereas ComR proteins
497 from Bovis and Pyogenic streptococci are more promiscuous in the XIP peptides that they are
498 able to recognize to enhance ComR DNA binding capacity. It is then a logical conclusion that
499 the Mutans group has further separated from the Bovis and Pyogenic group in terms of ComR-
500 XIP regulation. A logical extrapolation of these observations is to ask whether XrpA could serve
501 as a novel anti-carries target or therapeutic. It is important to note that other oral health-
502 associated commensal streptococci, such as *Streptococcus mitis*, *Streptococcus gordonii* and
503 *Streptococcus sanguinis* are all part of the Mitis group of streptococci that lack ComRS signaling
504 systems and rely on ComDE for competence activation (Håvarstein, 2010), so targeting XrpA
505 should not disrupt a healthy oral biofilm. It is encouraging that small synthesized portions of
506 XrpA have an effect on competence activation, as shown in Figure 4. It is critical to point out
507 that while these synthesized peptides were provided exogenously in this study, we do not
508 suspect at this time that XrpA is actively released to the extracellular environment. As previously
509 discussed, our current working hypothesis is that XrpA is able to accumulate in response to
510 external environmental cues, such as oxidative stress, and function as a sensor inside the cells,

511 and at this time have no reason to believe that XrpA has an extracellular lifecycle. Our working
512 model must also account for the fact that XrpA fragments can elicit effects when provided
513 exogenously. Therefore, we are testing the hypothesis that XrpA peptides, which may be
514 released into the extracellular space through lysis, can be actively internalized, perhaps after
515 processing, to elicit their effects on ComR – similar to what has been proposed for XIP (Kaspar
516 *et al.*, 2017). Mass spectrometry studies are currently ongoing to localize XrpA and other *S.*
517 *mutans* encoded peptides that affect competence (Ahn *et al.*, 2014).

518 In summary, this work provide additional novel insights into the complex regulatory
519 nature of bacterial cell-cell signaling systems, providing the organisms with multiple check
520 points throughout the circuit to either amplify or diminish the response to signal inputs based on
521 key environmental and/or physiologic cues. Future work will be focused on how environmental
522 inputs can influence XrpA/ComR interaction and activities, and the resulting consequences in
523 terms of biofilm ecology. Development of these model systems should shed further light on
524 microbial interactions and the importance of cell-cell signaling systems at the very earliest
525 stages of colonization and biofilm development. It is also interesting to ponder if the recently
526 discovered peptides such as XrpA, the *rcrQ*-associated peptides of *S. mutans* (Ahn *et al.*, 2014)
527 and the leaderless SHP of GAS (Do *et al.*, 2017) play important roles in the virulence potential
528 of these organisms if multiple other peptides with profound impacts on cellular behaviors are
529 currently hidden in the genomes of Gram-positive bacteria.

530

531 **EXPERIMENTAL PROCEDURES**

532 *Bacterial Strains and Growth Conditions.*

533 *S. mutans* wild-type strain UA159 and its derivatives (**Table 1**) were grown in either brain heart
534 infusion (BHI - Difco), FMC (Terleckyj *et al.*, 1975; Terleckyj and Shockman, 1975) or CDM
535 (Chang *et al.*, 2011) medium. The medium was supplemented with 10 $\mu\text{g ml}^{-1}$ erythromycin, 1
536 mg ml^{-1} of kanamycin or 1 mg ml^{-1} spectinomycin when needed. Unless otherwise noted,
537 cultures were grown overnight in BHI medium with the appropriate antibiotics at 37°C in a 5%
538 CO₂ aerobic atmosphere. The next day, cultures were harvested by centrifugation, washed
539 twice in 1 mL of phosphate-buffered saline (PBS), and resuspended in PBS to remove all traces
540 of BHI. Cells were then diluted in the desired medium before beginning each experiment.
541 Synthetic XIP (sXIP, aa sequence = GLDWWSL), corresponding to residues 11-17 of ComS,
542 was synthesized and purified to 96% homogeneity by NeoBioSci (Cambridge, MA). The
543 lyophilized sXIP was reconstituted with 99.7% dimethyl sulfoxide (DMSO) to a final
544 concentration of 2 mM and stored in 100 μL aliquots at -20°C. Selected XrpA peptide
545 sequences and fluorescently-labeled derivatives were synthesized, purified and confirmed by
546 mass spectrometry by Biomatik USA (Wilmington, DE). For scrambled peptides, the Shuffle
547 Protein tool from www.bioinformatics.org was utilized. XrpA peptides were also reconstituted
548 with DMSO to a final concentration of 1 mM and stored at -20°C.

549

550 *Construction of Bacterial Strains.*

551 Mutant strains of *S. mutans*, including inactivation of the *xrpA* start codon ($\Delta xrpA$) were created
552 using a PCR ligation mutagenesis approach as previously described (Lau *et al.*, 2002; Kaspar *et*
553 *al.*, 2015). Overexpression of genes (*xrpA*, *comR*) was achieved by amplifying the structural
554 genes of interest from *S. mutans* UA159 and cloning into the expression plasmid pIB184 using
555 the EcoRI and BamHI restriction sites (Biswas *et al.*, 2008). For *in vivo* protein-protein
556 interaction experiments, a Strep-tag sequencing (WSHPQFEK) was first inserted in front of the

557 stop codon on the pIB184-ComR overexpressing plasmid using the Q5® Site Directed
558 Mutagenesis Kit (New England Biolabs, Beverly, Mass.) and following the provided protocol.
559 After selection of the appropriate construct by sequencing, a [G4S]₂ Linker sequence
560 (ggtggaggaggctctggtggaggcggtagc) was then inserted between the *comR* and Strep-tag
561 sequence using the same kit and protocol (**Supplemental Table 1**). Transformants were
562 confirmed by PCR and sequencing after selection on BHI agar with appropriate antibiotics.
563 Plasmid DNA was isolated from *E. coli* using QIAGEN (Chatsworth, Calif.) miniprep columns,
564 and restriction and DNA-modifying enzymes were obtained from New England Biolabs. PCRs
565 were carried out with 100 ng of chromosomal DNA by using *Taq* DNA polymerase, and PCR
566 products were purified with the QIAquick kit (QIAGEN).

567

568 *Transcriptome Profiling via RNA-Seq.*

569 Selected strains of *S. mutans* to be analyzed by RNA-sequencing (UA159, $\Delta xrpA$) were grown
570 in FMC medium to mid-exponential log phase of OD₆₀₀ = 0.5 before harvesting. For *S. mutans*
571 UA159 treated with 2 μ M sXIP, sXIP was added at OD₆₀₀ = 0.2. RNA extraction, rRNA removal,
572 library construction and read analysis was conducted as previously described elsewhere (Zeng
573 *et al.*, 2013; Kaspar *et al.*, 2015). Briefly, 10 μ g of high-quality total RNA was processed using
574 the MICROBExpress™ Bacterial mRNA Enrichment Kit (Ambion of Life Technologies, Grand
575 Island, NY), twice, before ethanol precipitation and resuspension in 25 μ L of nuclease-free
576 water. The quality of enriched mRNA samples was analyzed using an Agilent Bioanalyzer
577 (Agilent Technologies, Santa Clara, CA). cDNA libraries were generated from the enriched
578 mRNA samples using the TruSeq Illumina kit (Illumina, San Diego, CA), following instructions
579 from the supplier. Deep sequencing was performed at the University of Florida ICBR facilities
580 (Gainesville, FL). Approximately 20 million short-reads were obtained for each sample. After
581 removing adapter sequences from each short-read and trimming of the 3'-ends by quality

582 scores (Schmieder and Edwards, 2011), the resulting sequences were mapped onto the
583 reference genome of strain UA159 (GenBank accession no. AE014133) using the short-read
584 aligner. Mapped short-read alignments were then converted into readable formats using
585 SAMTOOLS (Li *et al.*, 2009). For viewing of the mapped reads aligned to the genome, .bam
586 files were uploaded into the Integrative Genomics Viewer (IGV – version 2.3.55) (Robinson *et*
587 *al.*, 2011). A “.csv” file containing raw read counts for each replicate (3) was then uploaded to
588 Degust (<http://degust.erc.monash.edu/>) and edgeR analysis performed to determine Log2 fold
589 change and a false discovery rate (FDR). The P-value was obtained by taking the $-\log_{10}$ of the
590 FDR. The data files used in this study are available from NCBI-GEO (Gene Expression
591 Omnibus) under accession no. GSE110167.

592

593 *Measurements of Promoter Activity via GFP Fluorescence.*

594 For measurements of GFP fluorescence, cultures were inoculated from washed overnight
595 cultures in CDM medium at a 1:50 dilution. Inoculated medium (175 μ L) was added to each well
596 along with a 50 μ L mineral oil overlay in a Costar™ 96 well assay plate (black plate with clear
597 bottom; Corning Incorporated) and incubated at 37°C. At intervals of 30 minutes for a total of 18
598 hours, OD₆₀₀ along with GFP fluorescence (excitation 485/20 nm, emission 528/20 nm) was
599 measured with a Synergy 2 multimode microplate reader (BioTek). Relative expression was
600 calculated by subtracting the background fluorescence of UA159 (mean from six replicates)
601 from raw fluorescence units of the reporter strains and then dividing by OD₆₀₀.

602

603 *Flow cytometry.*

604 Bacterial cultures were grown to OD₆₀₀ = 0.6 before being harvested, washed and resuspended
605 in PBS before being run through a FACSCalibur™ (BD Biosciences) flow cytometer. For sCSP
606 experiments, cultures were grown in BHI after a 1:20 dilution from overnight culture while

607 cultures were grown in FMC for sXIP experiments at the same initial dilution. Both peptides
608 were added to the growing cultures at $OD_{600} = 0.2$. sXIP treated cells were stained with $5 \mu\text{g}$
609 mL^{-1} propidium iodide (PI) for 10 minutes in the dark for analysis of membrane-compromised
610 cells. Cells were then sonicated in a water bath sonicator for 3 intervals of 30 seconds in 5 mL
611 polystyrene round-bottom tubes to achieve primarily single cells for analysis. Forward and side
612 scatter signals were set stringently to allow sorting of single cells. In total, 5×10^4 cells were
613 counted from each event, at a maximum rate of 2×10^3 cells per second, and each experiment
614 was performed in triplicate. Detection of GFP fluorescence was through a 530 nm (± 30 nm)
615 bandpass filter, and PI was detected using a 670-nm long pass filter. Data were acquired for
616 unstained cells and single-color positive controls so that data collection parameters could be
617 properly set. The data were collected using Cell Quest Pro (BD Biosciences) and analyzed with
618 FCS Express 4 (De Novo Software). Gating for quadrant analysis was selected by using a dot
619 density plot with forward and side scatter, with gates set to capture the densest section of the
620 plot. Graphing and statistical analyses were performed using Prism (GraphPad Software). x-
621 and y-axis data represent logarithmic scales of fluorescent intensity (arbitrary units).

622

623 *Measurements of eDNA Release.*

624 Overnight cultures of selected *S. mutans* strains, grown in CDM medium with addition of a final
625 concentration of $10 \mu\text{M}$ of synthetic XrpA peptides when noted, were measured for a final
626 OD_{600} and then harvested by centrifugation for their supernatant fraction. 5 mL of the resulting
627 supernatant was then run through QIAGEN (Chatsworth, Calif.) PCR purification columns to
628 capture eDNA present. The eDNA was then eluted off the column with $600 \mu\text{L}$ water, and 594
629 μL of this elution was mixed with $5 \mu\text{L}$ of $50 \mu\text{M}$ Sytox Green (Invitrogen) to a final concentration
630 of $0.5 \mu\text{M}$. After vortexing the solution and incubation for 15 minutes in the dark at room
631 temperature, $200 \mu\text{L}$ of the stained samples were transferred into a Costar™ 96 well assay plate
632 (black plate with clear bottom; Corning Incorporated). Fluorescence (excitation 485/20 nm,

633 emission 528/20 nm) was measured with a Synergy 2 multimode microplate reader (BioTek)
634 and the resulting data was then normalized for the measured final OD₆₀₀ nm resulting in a final
635 arbitrary eDNA release measurement. The data represents 3 independent biological replicates
636 with 3 technical replicates each. Statistical significance was determined by the Student's T-Test.

637

638 *Biofilm Assays.*

639 Selected *S. mutans* strains were grown from overnight cultures to mid-exponential phase after a
640 1:20 dilution in BHI broth at 37°C in a 5% CO₂ atmosphere. The mid-exponential phase cells
641 were then diluted 1:100 into CDM medium with containing 15 mM glucose and 2.5 mM sucrose
642 as a carbohydrate source. 200 µL of this dilution was loaded into 96 well polystyrene microtiter
643 plates and incubated in a 5% CO₂ atmosphere at 37°C for 48 h. After, the medium was
644 decanted, and the plates were washed twice with 200 µL of sterile water to remove planktonic
645 and loosely bound cells. The adherent bacteria were stained with 60 µL of 0.1% crystal violet for
646 15 min. After rinsing twice with 200 µL of water, the bound dye was extracted from the stained
647 biofilm using 200 µL of ethanol:acetone (8:2) solution, twice. The extracted dye was diluted into
648 1.6 mL of ethanol:acetone solution. Biofilm formation was quantified by measuring the
649 absorbance of the solution at OD₅₇₅ nm. The data represents 3 independent biological
650 replicates with 4 technical replicates each. Statistical significance was determined by the
651 Student's T-Test.

652

653 *SPINE for ComR Interactions.*

654 A Strep-tag protein interaction experiment (SPINE) was derived from a previously published
655 protocol (Herzberg *et al.*, 2007). Briefly, a strain harboring a C-terminal Strep-tagged ComR,
656 along with the vector only control, was grown in 500 mL of CDM medium after a 1:20 dilution
657 from overnight cultures to an OD₆₀₀ = 0.6. At this time, either 2 µM of sXIP or DMSO (vehicle,
658 0.1% final concentration) was added to cultures and were grown an additional hour at 37°C in a

659 5% CO₂ atmosphere. After, cells were pelleted by centrifugation, washed and resuspended in 50
660 mM HEPES (pH 8) with a final concentration of 2.5 mM of protein crosslinker solution added
661 (DSP, Thermo Scientific). The cells were incubated at 37°C for 45 minutes, at which point 50
662 mM Tris (pH 7.5) was added to stop the crosslinking reaction. After, cells were pelleted, washed
663 in Buffer W, and lysed via bead beating in Buffer W. The crosslinked Strep-tagged ComR
664 complex was then purified from the lysate using Strep-tactin® resin (iba) in a chromatography
665 column following the manufacture's protocol. Purification was verified by running the selected
666 fractions and elutions on 16.5% Tris-Tricine gels (BioRad) followed by silver staining and/or
667 western blot (**Supplemental Figure 1**). Protein concentrations of the elutions were determined
668 using the bicinchoninic acid assay (BCA; Thermo Scientific). Complex-containing elutions were
669 then combined and precipitated by the TCA/Acetone precipitation method. Precipitant was sent
670 to Applied Biomics (Hayward, CA) for 2D DIGE Protein Expression Profiling which included 2D
671 gel electrophoresis, determination of protein expression ratios between samples, spot picking
672 and identification by LC-MS/MS though trypsin digestion of selected spots then returned peptide
673 fragments compared to a list of predicted masses using a *S. mutans* UA159 database of all
674 annotated proteins.

675

676 *Transformation Assays.*

677 Overnight cultures were diluted 1:20 in 200 µL of FMC medium in polystyrene microtiter plates
678 in the presence or absence of 10 µM of synthetic XrpA peptides. The cells were grown to OD₆₀₀
679 = 0.15 in a 5% CO₂ atmosphere. When desired, 0.5 µM of sXIP was added, cells were
680 incubated for 10 min and 0.5 µg of purified plasmid pIB184, which harbors a erythromycin
681 resistance (Erm^R) gene, was added to the culture. After 2.5 h incubation at 37°C, transformants
682 and total CFU were enumerated by plating appropriate dilutions on BHI agar plates with and
683 without the addition of 1 mg mL⁻¹ erythromycin, respectively. CFU were counted after 48 h of
684 incubation, and transformation efficiency was expressed as the percentage of transformants

685 among the total viable cells. Fold change was then calculated from the UA159 control with
686 DMSO (vehicle) addition. Statistical significance was determined by the Student's T-Test
687
688 *Western blot.*
689 Overnight cultures of *S. mutans* were diluted 1:50 into 35 mL of FMC medium and harvested by
690 centrifugation when the cultures reached an $OD_{600} = 0.5$. When desired, 2 μM sXIP was added
691 when the cultures reached an OD_{600} value of 0.2 along with 10 μM of selected XrpA peptides.
692 Cell pellets collected by centrifugation were washed once with buffer A (0.5 M sucrose; 10 mM
693 Tris-HCl, pH 6.8; 10 mM MgSO_4) containing 10 $\mu\text{g mL}^{-1}$ of phenylmethanesulfonyl fluoride
694 (PMSF) (ICN Biomedicals Inc.) and resuspended in 0.5 mL Tris-buffered saline (50 mM Tris-
695 HCl, pH 7.5; 150 mM NaCl). Cells were lysed using a Mini Bead Beater (Biospec Products) in
696 the presence of 1 volume of glass beads (avg. diam. 0.1 mm) for 30 s intervals, three times,
697 with incubation on ice between homogenizations. Lysates were then centrifuged at $3,000 \times g$ for
698 10 minutes at 4°C . Protein concentrations of the resulting supernates were determined using
699 the bicinchoninic acid assay (BCA; Thermo Scientific) with purified bovine serum albumin as the
700 standard. Ten microgram aliquots of proteins were mixed with 5X SDS sample buffer (200 mM
701 Tris-HCl, pH 6.8; 10% [v/v] SDS; 20% [v/v]; 10% [v/v] β -mercaptoethanol; 0.02% [v/v]
702 bromophenol blue), loaded on a 12.5% polyacrylamide gel with a 5% stacking gel and
703 separated by electrophoresis at 150 V for 45 minutes. Proteins were transferred to Immobilon-P
704 polyvinylidene difluoride (PVDF) membranes (Millipore) using a Trans-Blot Turbo transfer
705 system and a protocol provided by the supplier (BioRad). The membranes were treated with
706 either primary polyclonal anti-ComX, anti-ComR or anti-ManL (loading control) antisera at a
707 1:1000 dilution and a secondary peroxidase-labeled, goat anti-rabbit IgG antibody (1:5000
708 dilution; Kierkegaard & Perry Laboratories, USA). Detection was performed using a SuperSignal
709 West Pico Chemiluminescent Substrate kit (Thermo Scientific) and visualized with a FluorChem
710 8900 imaging system (Alpha Innotech, USA).

711

712 *Purification of Recombinant ComR.*

713 The *S. mutans* UA159 *comR* gene was amplified using primers AAAGAATCCTATGTTAAAAGA
714 and CACCCTAGGAGACCCATCAAAA and was cloned into the BamHI and AvrII sites of the pET
715 45b expression vector downstream of the 6x His-tag and separated by an enterokinase
716 cleavage site. The resulting vector was transformed into *E. coli* DE3 cells (New England
717 Biolabs). To induce expression of *comR*, 1 mM isopropyl- β -D-thiogalactopyranoside (IPTG) was
718 added to 1 L of growing culture in LB medium once the OD₆₀₀ reached 0.6. The culture was
719 grown for an additional 4 h at 37°C before the cells were pelleted by centrifugation and frozen
720 overnight at -20°C. The next day, the cells were lysed after suspension into B-PER (Thermo
721 Scientific) with addition of HALT protease inhibitor (Thermo Scientific) and cellular debris
722 removed by centrifugation for 20 minutes at 13,000 x g. The His-ComR was column purified
723 using Ni-NTA resin (QIAGEN) and eluted with 250 mM imidazole (**Supplemental Figure 4**). To
724 remove the 6x His-tag, 1 mL of a 2-3 mg mL⁻¹ purified His-ComR sample was dialyzed in
725 EKMax Buffer overnight (50 mM Tris-HCL pH 8, 1 mM CaCl₂, 0.1% Tween-20) with 50 U of
726 EKMax enterokinase (Thermo Scientific) then added and incubated overnight at 4°C. Finally,
727 the cleaved ComR sample was added to a dialysis cassette to exchange the EKMax buffer with
728 PBS pH 7.4 overnight. Final protein concentration was determined using the bicinchoninic acid
729 assay (BCA; Thermo Scientific) with purified bovine serum albumin as the standard. Digestion
730 was confirmed by SDS-PAGE and Coomassie Blue staining (**Supplemental Figure 5**).

731

732 *Fluorescence Polarization*

733 A 5' Bodipy-labeled self-annealing, stem-loop DNA probe with sequence encompassing the
734 ECom-box which ComR binds to within the *PcomX* promoter (5'-BODIPY FL-X -
735 ATGGGACATTTATGTCCTGTCCCCACAGGACATAAATGTCCCAT - 3'), was synthesized
736 (Thermo Fisher) and kept at a constant concentration of 1 μ M in all reactions. Purified ComR

737 protein was serially diluted, ranging from 5 to 2000 nM, and mixed with 10 μ M sXIP and 10 μ M
738 of selected synthetic XrpA peptides unless otherwise noted, in reaction buffer to a final volume
739 of 250 μ L (PBS pH 7.4, 10 mM β ME, 1 mM EDTA, 0.1 mg mL⁻¹ BSA, 20% glycerol (v/v), 0.01%
740 Triton X-100 and 0.05 mg mL⁻¹ salmon sperm DNA). Reactions were transferred to a Corning®
741 96-well, half-area, black polystyrene plate prior to incubation at 37°C for 30 minutes.
742 Polarization values were measured using a BioTek Synergy 2 plate reader (excitation 485 nm,
743 emission 528 nm), and the resulting millipolarization values were plotted for each protein
744 concentration tested to assess protein/peptide interactions. For fluorescent peptides
745 experiments, a synthetic fluorescein isothiocyanate (FITC)-labeled XrpA-N1 peptide (FITC-AHX-
746 MIQNCISILRHFLITLK) was used (Biomatik USA) with reaction buffer PBS pH 7.4, 10 mM β ME,
747 0.1 mg mL⁻¹ BSA, 20% glycerol (v/v), and 0.01% Triton X-100. Graphing and linear regression
748 analyses to determine kD values were performed using Prism (GraphPad Software).

749 **ACKNOWLEDGEMENTS**

750 Research reported in this publication was supported by the National Institute of Dental and
751 Craniofacial Research of the National Institutes of Health under Award Numbers R01 DE13239,
752 R01 DE023339, and T90 DE21990.

753

754 **AUTHOR CONTRIBUTIONS**

755 JK, RCS and RAB contributed to the conception and design of the study; JK and RCS

756 performed the experiments, acquired and analyzed the data, JK and RAB interpreted the data;

757 and JK and RAB wrote the manuscript.

758

759 **REFERENCES**

- 760 Abranches, J., Nascimento, M.M., Zeng, L., Browngardt, C.M., Wen, Z.T., Rivera, M.F., and
761 Burne, R.A. (2008) CcpA regulates central metabolism and virulence gene expression in
762 *Streptococcus mutans*. *J Bacteriol* **190**: 2340–9
763
- 764 Ahn, S.-J., Kaspar, J., Kim, J.N., Seaton, K., and Burne, R. a (2014) Discovery of novel peptides
765 regulating competence development in *Streptococcus mutans*. *J Bacteriol* **196**: 3735–3745.
766
- 767 Ahn, S.-J., and Rice, K.C. (2016) Understanding the *Streptococcus mutans* Cid/Lrg System
768 through CidB Function. *Appl Environ Microbiol* **82**: 6189–6203.
769
- 770 Ahn, S.-J., Wen, Z.T., and Burne, R.A. (2007) Effects of oxygen on virulence traits of
771 *Streptococcus mutans*. *J Bacteriol* **189**: 8519–27.
772
- 773 Biswas, I., Jha, J.K., and Fromm, N. (2008) Shuttle expression plasmids for genetic studies in
774 *Streptococcus mutans*. *Microbiology* **154**: 2275–82.
775
- 776 Boutry, C., Delplace, B., Clippe, A., Fontaine, L., and Hols, P. (2013) SOS response activation
777 and competence development are antagonistic mechanisms in *Streptococcus thermophilus*. *J*
778 *Bacteriol* **195**: 696–707.
779
- 780 Bowen, W.H., Burne, R.A., Wu, H., and Koo, H. (2017) Oral Biofilms: Pathogens, Matrix, and
781 Polymicrobial Interactions in Microenvironments. *Trends Microbiol*
782 <https://doi.org/10.1016/j.tim.2017.09.008>.
783
- 784 Chandrangu, P., Lemke, J.J., and Gourse, R.L. (2011) The *dksA* promoter is negatively

- 785 feedback regulated by DksA and ppGpp. *Mol Microbiol* **80**: 1337–48.
- 786
- 787 Chang, J.C., and Federle, M.J. (2016) PptAB Exports Rgg Quorum-Sensing Peptides in
788 *Streptococcus*. *PLoS One* **11**: e0168461.
- 789
- 790 Chang, J.C., LaSarre, B., Jimenez, J.C., Aggarwal, C., and Federle, M.J. (2011) Two Group A
791 Streptococcal Peptide Pheromones Act through Opposing Rgg Regulators to Control Biofilm
792 Development. *PLoS Pathog* **7**: e1002190.
- 793
- 794 Chatteraj, P., Banerjee, A., Biswas, S., and Biswas, I. (2010) ClpP of *Streptococcus mutans*
795 differentially regulates expression of genomic islands, mutacin production, and antibiotic
796 tolerance. *J Bacteriol* **192**: 1312–23.
- 797
- 798 Desai, K., Mashburn-Warren, L., Federle, M.J., and Morrison, D.A. (2012) Development of
799 competence for genetic transformation of *Streptococcus mutans* in a chemically defined
800 medium. *J Bacteriol* **194**: 3774–80.
- 801
- 802 Do, H., Makthal, N., VanderWal, A.R., Rettel, M., Savitski, M.M., Peschek, N., *et al.* (2017)
803 Leaderless secreted peptide signaling molecule alters global gene expression and increases
804 virulence of a human bacterial pathogen. *Proc Natl Acad Sci U S A* **114**: E8498–E8507.
- 805
- 806 Fontaine, L., Boutry, C., Frahan, M.H. de, Delplace, B., Fremaux, C., Horvath, P., *et al.* (2009) A
807 Novel Pheromone Quorum-Sensing System Controls the Development of Natural Competence
808 in *Streptococcus thermophilus* and *Streptococcus salivarius*. *J Bacteriol* **192**: 1444–1454.
- 809
- 810 Fontaine, L., Goffin, P., Dubout, H., Delplace, B., Baulard, A., Lecat-Guillet, N., *et al.* (2013)

811 Mechanism of competence activation by the ComRS signalling system in streptococci. *Mol*
812 *Microbiol* **87**: 1113–32.

813

814 Fuqua, W.C., Winans, S.C., and Greenberg, E.P. (1994) Quorum sensing in bacteria: the LuxR-
815 LuxI family of cell density-responsive transcriptional regulators. *J Bacteriol* **176**: 269–75.

816

817 Furio, M. De, Ahn, S.J., Burne, R.A., and Hagen, S.J. (2017) Oxidative Stressors Modify the
818 Response of *Streptococcus mutans* to Its Competence Signal Peptides. *Appl Environ Microbiol*
819 **83**: e01345-17.

820

821 Gamba, P., Jonker, M.J., and Hamoen, L.W. (2015) A Novel Feedback Loop That Controls
822 Bimodal Expression of Genetic Competence. *PLoS Genet* **11**: e1005047.

823

824 Gardan, R., Besset, C., Gitton, C., Guillot, A., Fontaine, L., Hols, P., and Monnet, V. (2013)
825 Extracellular life cycle of ComS, the competence-stimulating peptide of *Streptococcus*
826 *thermophilus*. *J Bacteriol* **195**: 1845–55.

827

828 Greenberg, E.P. (2003) Bacterial communication and group behavior. *J Clin Invest* **112**: 1288–
829 90.

830

831 Guo, Q., Ahn, S.-J., Kaspar, J., Zhou, X., and Burne, R.A. (2014) Growth phase and pH
832 influence peptide signaling for competence development in *Streptococcus mutans*. *J Bacteriol*
833 **196**: 227–36.

834

835 Hagen, S.J., and Son, M. (2017) Origins of heterogeneity in *Streptococcus mutans* competence:
836 interpreting an environment-sensitive signaling pathway. *Phys Biol* **14**: 15001.

837 Haustenne, L., Bastin, G., Hols, P., and Fontaine, L. (2015) Modeling of the ComRS Signaling
838 Pathway Reveals the Limiting Factors Controlling Competence in *Streptococcus thermophilus*.
839 *Front Microbiol* **6**.
840
841 Håvarstein, L.S. (2010) Increasing competence in the genus *Streptococcus*. *Mol Microbiol* **78**:
842 541–4.
843
844 Håvarstein, L.S., Coomaraswamy, G., and Morrison, D.A. (1995) An unmodified
845 heptadecapeptide pheromone induces competence for genetic transformation in *Streptococcus*
846 *pneumoniae*. *Proc Natl Acad Sci U S A* **92**: 11140–4.
847
848 Herzberg, C., Weidinger, L.A.F., Dörrbecker, B., Hübner, S., Stülke, J., and Commichau, F.M.
849 (2007) SPINE: A method for the rapid detection and analysis of protein–protein interactions in
850 vivo. *Proteomics* **7**: 4032–4035.
851
852 Hui, F.M., Zhou, L., and Morrison, D.A. (1995) Competence for genetic transformation in
853 *Streptococcus pneumoniae*: organization of a regulatory locus with homology to two lactococcal
854 A secretion genes. *Gene* **153**: 25–31.
855
856 Hung, D.C.I., Downey, J.S., Ayala, E.A., Kreth, J., Mair, R., Senadheera, D.B., *et al.* (2011)
857 Characterization of DNA binding sites of the ComE response regulator from *Streptococcus*
858 *mutans*. *J Bacteriol* **193**: 3642–52.
859
860 Johnston, C., Martin, B., Fichant, G., Polard, P., and Claverys, J.-P. (2014) Bacterial
861 transformation: distribution, shared mechanisms and divergent control. *Nat Rev Microbiol* **12**:
862 181–96.

- 863 Kaspar, J., Ahn, S.-J., Palmer, S.R., Choi, S.C., Stanhope, M.J., and Burne, R.A. (2015) A
864 Unique ORF within the *comX* gene of *Streptococcus mutans* Regulates Genetic Competence
865 and Oxidative Stress Tolerance. *Mol Microbiol* **96**: 463–482.
- 866
- 867 Kaspar, J., Kim, J.N., Ahn, S.-J., and Burne, R.A. (2016) An Essential Role for (p)ppGpp in the
868 Integration of Stress Tolerance, Peptide Signaling, and Competence Development in
869 *Streptococcus mutans*. *Front Microbiol* **7**: 1162.
- 870
- 871 Kaspar, J., Underhill, S.A.M., Shields, R.C., Reyes, A., Rosenzweig, S., Hagen, S.J., and
872 Burne, R.A. (2017) Intercellular communication via the *comX*-Inducing Peptide (XIP) of
873 *Streptococcus mutans*. *J Bacteriol* JB.00404-17.
- 874
- 875 Khan, R., Rukke, H. V., Høvik, H., Åmdal, H.A., Chen, T., Morrison, D.A., and Petersen, F.C.
876 (2016) Comprehensive Transcriptome Profiles of *Streptococcus mutans* UA159 Map Core
877 Streptococcal Competence Genes. *mSystems* **1**: e00038-15.
- 878
- 879 Khan, R., Rukke, H. V, Ricomini Filho, A.P., Fimland, G., Arntzen, M.Ø., Thiede, B., and
880 Petersen, F.C. (2012) Extracellular identification of a processed type II ComR/ComS
881 pheromone of *Streptococcus mutans*. *J Bacteriol* **194**: 3781–8.
- 882
- 883 Kreth, J., Hung, D.C.I., Merritt, J., Perry, J., Zhu, L., Goodman, S.D., *et al.* (2007) The response
884 regulator ComE in *Streptococcus mutans* functions both as a transcription activator of mutacin
885 production and repressor of CSP biosynthesis. *Microbiology* **153**: 1799–807.
- 886
- 887 Lau, P.C., Sung, C.K., Lee, J.H., Morrison, D.A., and Cvitkovitch, D.G. (2002) PCR ligation
888 mutagenesis in transformable streptococci: application and efficiency. *J Microbiol Methods* **49**:

889 193–205.

890

891 LeBlanc, D.J., Lee, L.N., and Abu-Al-Jaibat, A. (1992) Molecular, genetic, and functional
892 analysis of the basic replicon of pVA380-1, a plasmid of oral streptococcal origin. *Plasmid* **28**:
893 130–145.

894

895 Lemos, J.A., Quivey, R.G., Koo, H., and Abranches, J. (2013) *Streptococcus mutans*: a new
896 Gram-positive paradigm? *Microbiology* **159**: 436–45.

897

898 Li, H., Handsaker, B., Wysoker, A., Fennell, T., Ruan, J., Homer, N., *et al.* (2009) The Sequence
899 Alignment/Map format and SAMtools. *Bioinformatics* **25**: 2078–9.

900

901 Li, Y.H., Lau, P.C., Lee, J.H., Ellen, R.P., and Cvitkovitch, D.G. (2001) Natural genetic
902 transformation of *Streptococcus mutans* growing in biofilms. *J Bacteriol* **183**: 897–908.

903

904 Liao, S., Klein, M.I., Heim, K.P., Fan, Y., Bitoun, J.P., Ahn, S.-J., *et al.* (2014) *Streptococcus*
905 *mutans* extracellular DNA is upregulated during growth in biofilms, actively released via
906 membrane vesicles, and influenced by components of the protein secretion machinery. *J*
907 *Bacteriol* **196**: 2355–66.

908

909 Martin, B., Soulet, A.-L., Mirouze, N., Prudhomme, M., Mortier-Barrière, I., Granadel, C., *et al.*
910 (2013) ComE/ComE~P interplay dictates activation or extinction status of pneumococcal X-state
911 (competence). *Mol Microbiol* **87**: 394–411.

912

913 Mashburn-Warren, L., Morrison, D.A., and Federle, M.J. (2010) A novel double-tryptophan

- 914 peptide pheromone controls competence in *Streptococcus* spp. via an Rgg regulator. *Mol*
915 *Microbiol* **78**: 589–606.
- 916
- 917 Mashburn-Warren, L., Morrison, D.A., and Federle, M.J. (2012) The cryptic competence
918 pathway in *Streptococcus pyogenes* is controlled by a peptide pheromone. *J Bacteriol* **194**:
919 4589–600.
- 920
- 921 Mirouze, N., Bergé, M.A., Soulet, A.-L., Mortier-Barrière, I., Quentin, Y., Fichant, G., *et al.*
922 (2013) Direct involvement of DprA, the transformation-dedicated RecA loader, in the shut-off of
923 pneumococcal competence. *Proc Natl Acad Sci U S A* **110**: E1035-44.
- 924
- 925 Moye, Z.D., Son, M., Rosa-Alberty, A.E., Zeng, L., Ahn, S.-J., Hagen, S.J., and Burne, R.A.
926 (2016) Effects of Carbohydrate Source on Genetic Competence in *Streptococcus mutans*. *Appl*
927 *Environ Microbiol* AEM.01205-16.
- 928
- 929 Okamoto, M., Imai, S., Miyanohara, M., Saito, W., Momoi, Y., Abo, T., *et al.* (2013)
930 *Streptococcus troglodytae* sp. nov., from the chimpanzee oral cavity. *Int J Syst Evol Microbiol*
931 **63**: 418–422.
- 932
- 933 Papenfort, K., and Bassler, B.L. (2016) Quorum sensing signal–response systems in Gram-
934 negative bacteria. *Nat Rev Microbiol* **14**: 576–588.
- 935
- 936 Perry, J.A., Jones, M.B., Peterson, S.N., Cvitkovitch, D.G., and Lévesque, C.M. (2009) Peptide
937 alarmone signalling triggers an auto-active bacteriocin necessary for genetic competence. *Mol*
938 *Microbiol* **72**: 905–17.
- 939

- 940 Robinson, J.T., Thorvaldsdóttir, H., Winckler, W., Guttman, M., Lander, E.S., Getz, G., and
941 Mesirov, J.P. (2011) Integrative genomics viewer. *Nat Biotechnol* **29**: 24–6.
- 942
- 943 Schmieder, R., and Edwards, R. (2011) Quality control and preprocessing of metagenomic
944 datasets. *Bioinformatics* **27**: 863–4.
- 945
- 946 Shanker, E., Morrison, D.A., Talagas, A., Nessler, S., Federle, M.J., and Prehna, G. (2016)
947 Pheromone Recognition and Selectivity by ComR Proteins among *Streptococcus* Species.
948 *PLoS Pathog* **12**: e1005979.
- 949
- 950 Shields, R.C., and Burne, R.A. (2016) Growth of *Streptococcus mutans* in Biofilms Alters
951 Peptide Signaling at the Sub-population Level. *Front Microbiol* **7**: 1075.
- 952
- 953 Son, M., Ahn, S.-J., Guo, Q., Burne, R.A., and Hagen, S.J. (2012) Microfluidic study of
954 competence regulation in *Streptococcus mutans*: environmental inputs modulate bimodal and
955 unimodal expression of *comX*. *Mol Microbiol* **86**: 258–72.
- 956
- 957 Son, M., Ghoreishi, D., Ahn, S.-J., Burne, R.A., and Hagen, S.J. (2015) Sharply Tuned pH
958 Response of Genetic Competence Regulation in *Streptococcus mutans*: a Microfluidic Study of
959 the Environmental Sensitivity of *comX*. *Appl Environ Microbiol* **81**: 5622–31.
- 960
- 961 Straume, D., Stamsås, G.A., and Håvarstein, L.S. (2015) Natural transformation and genome
962 evolution in *Streptococcus pneumoniae*. *Infect Genet Evol* **33**: 371–80.
- 963
- 964 Talagas, A., Fontaine, L., Ledesma-Garca, L., Mignolet, J., Li de la Sierra-Gallay, I., Lazar, N.,
965 *et al.* (2016) Structural Insights into Streptococcal Competence Regulation by the Cell-to-Cell

- 966 Communication System ComRS. *PLOS Pathog* **12**: e1005980.
- 967
- 968 Terleckyj, B., and Shockman, G.D. (1975) Amino acid requirements of *Streptococcus mutans*
969 and other oral streptococci. *Infect Immun* **11**: 656–664.
- 970
- 971 Terleckyj, B., Willett, N.P., and Shockman, G.D. (1975) Growth of several cariogenic strains of
972 oral streptococci in a chemically defined medium. *Infect Immun* **11**: 649–55.
- 973
- 974 Tomasz, A. (1965) Control of the Competent State in Pneumococcus by a Hormone-Like Cell
975 Product: An Example for a New Type of Regulatory Mechanism in Bacteria. *Nature* **208**: 155–
976 159.
- 977
- 978 Waterhouse, J.C., Swan, D.C., and Russell, R.R.B. (2007) Comparative genome hybridization
979 of *Streptococcus mutans* strains. *Oral Microbiol Immunol* **22**: 103–110.
- 980
- 981 Wei, H., and Håvarstein, L.S. (2012) Fratricide is essential for efficient gene transfer between
982 pneumococci in biofilms. *Appl Environ Microbiol* **78**: 5897–905.
- 983
- 984 Wenderska, I.B., Lukenda, N., Cordova, M., Magarvey, N., Cvitkovitch, D.G., and Senadheera,
985 D.B. (2012) A novel function for the competence inducing peptide, XIP, as a cell death effector
986 of *Streptococcus mutans*. *FEMS Microbiol Lett* **336**: 104–12.
- 987
- 988 Weng, L., Piotrowski, A., and Morrison, D.A. (2013) Exit from Competence for Genetic
989 Transformation in *Streptococcus pneumoniae* Is Regulated at Multiple Levels. *PLoS One* **8**:
990 e64197.
- 991

992 Whiteley, M., Diggle, S.P., and Greenberg, E.P. (2017) Progress in and promise of bacterial
993 quorum sensing research. *Nature* **551**: 313–320.

994

995 Wilkening, R. V., Chang, J.C., and Federle, M.J. (2016) PepO, a CovRS-controlled
996 endopeptidase, disrupts *Streptococcus pyogenes* quorum sensing. *Mol Microbiol* **99**: 71-87.

997

998 Zeng, L., Choi, S.C., Danko, C.G., Siepel, A., Stanhope, M.J., and Burne, R.A. (2013) Gene
999 regulation by CcpA and catabolite repression explored by RNA-Seq in *Streptococcus mutans*.

1000 *PLoS One* **8**: e60465.

1001

1002

1003 **TABLES**

1004 TABLE 1. List of strains

Strain or Plasmid	Relevant Characteristics	Source or Reference
<i>S. mutans</i> Strains		
UA159	Wild-type	ATCC 700610
$\Delta xrpA$	Inactivation of <i>xrpA</i> start codon; <i>comX</i> ::T162C	(Kaspar <i>et al.</i> , 2015)
184XrpA/UA159	UA159 harboring overexpression of <i>xrpA</i> on pIB184, Em ^R	(Kaspar <i>et al.</i> , 2015)
$\Delta comR$	<i>comR</i> (SMU.61) :: Em ^R	(Kaspar <i>et al.</i> , 2016)
$\Delta comX$	<i>comX</i> (SMU.1997) :: Em ^R	(Kaspar <i>et al.</i> , 2015)
PcomX::gfp/UA159	UA159 harboring <i>gfp</i> fluorescent reporter of PcomX	(Son <i>et al.</i> , 2012)
PcomX::gfp/ $\Delta xrpA$	$\Delta xrpA$ harboring <i>gfp</i> fluorescent reporter of PcomX	This study
PcomX::gfp/184XrpA	184XrpA/UA159 harboring <i>gfp</i> fluorescent reporter of PcomX	This study
PcomS::gfp/UA159	UA159 harboring <i>gfp</i> fluorescent reporter of PcomS	(Kaspar <i>et al.</i> , 2017)
PcomS::gfp/ $\Delta xrpA$	$\Delta xrpA$ harboring <i>gfp</i> fluorescent reporter of PcomS	This study
PcomS::gfp/184XrpA	184XrpA/UA159 harboring <i>gfp</i> fluorescent reporter of PcomS	This study
PcomX::gfp/ $\Delta comS$	$\Delta comS$ (<i>comS</i> :: Em ^R) harboring <i>gfp</i> fluorescent reporter of PcomX	(Son <i>et al.</i> , 2012)
PcomX::gfp/ $\Delta comS\Delta xrpA$	$\Delta comS$ in <i>comX</i> ::T162C harboring <i>gfp</i> fluorescent reporter of PcomX	This study
184ComR-Strep/UA159	UA159 harboring overexpression of <i>comR</i> with addition of (G4S) ₂ linker and Strep-tag on pIB184, Em ^R	This study
Plasmids		
pDL278	Escherichia coli - Streptococcus shuttle vector, Sp ^R	(LeBlanc <i>et al.</i> , 1992)
pIB184	Shuttle expression plasmid with the constitutive P23 promoter, Em ^R	(Biswas <i>et al.</i> , 2008)

1005 * Em, erythromycin; Sp, spectinomycin.

1006

1007 TABLE 2. ComR Kd from Fluorescent Polarization
1008

Peptide	Sequence	ComR Kd (nM)*
		153 ± 10
1	CISILRHVFLITLKM	651 ± 99
2	VSKKVRNVVLLIEC	198 ± 17
3	LMKKSRLNTVC	169 ± 12
4	IFYFVIVCLHINKV	165 ± 13
S1	LFKFTCVRLILIISHM	248 ± 38
S2	KKNVIECVSRVL	147 ± 11
N1	MIQNCISILRHVFLITLK	783 ± 204
N2	MFCVSKKVRNVVLLIECLMCK	400 ± 49

1009 *ComR Kd determined from fluorescent polarization experiment shown in Figure 7A-D

1010 **FIGURE LEGENDS**

1011 *Figure 1. Transcriptome Analysis of $\Delta xrpA$ and UA159 with sXIP addition.* Volcano plots of (A)
1012 $\Delta xrpA$ and (B) UA159 + 2 μM sXIP from RNA-Seq results compared to UA159 of three
1013 independent replicates grown in FMC medium to $\text{OD}_{600} = 0.5$. Log₂ fold change and false
1014 discovery rates (FDR) converted to $-\log_{10}$ P-values were calculated from Degust using edgeR
1015 analysis. Genes of interest that were ≥ 1.5 log₂ fold change and had a ≥ 4 $-\log_{10}$ P-value were
1016 highlighted either in red (upregulated) or blue (downregulated) and are listed in Tables S2 and
1017 S3. (C) Visual representation of read counts accumulated in either the *comS*, *comX* or *comY*
1018 coding sequences in either the UA159 (blue bars) or $\Delta xrpA$ (orange bars) genetic backgrounds.
1019 Mapped short read alignments were converted in “.bam” files and visualized with the IGV
1020 genome browser.

1021
1022 *Figure 2. Effect of XrpA on activation of comX and comS promoters.* Transcriptional activation
1023 assays using a fused-*gfp* reporter for (A) *PcomX* and (B) *PcomS* in wild-type (UA159 – green
1024 circles), *comX*::T162C ($\Delta xrpA$ – blue squares) or *xrpA* overexpression (184XrpA – orange
1025 diamonds) genetic backgrounds. Black lines represent growth (OD_{600} , right axis) of each of the
1026 respective reporter strains during the assay. Each data point shown is the average of three
1027 independent biological replicates with four measured technical replicates.

1028
1029 *Figure 3. XrpA changes subpopulation behaviors.* Histogram of cell counts from flow cytometry
1030 analysis of the *PcomX*::*gfp* reporter strain in UA159 (black lines) or $\Delta xrpA$ (red lines) grown in
1031 BHI with addition of either (A) 100 nM or (B) 1000 nM sCSP. For experiments with FMC and
1032 addition of 2 μM sXIP, reporter strains in either (C) UA159 or (D) $\Delta comS$ background were
1033 stained with propidium iodide before analysis. A total of 50,000 cells were counted in three
1034 independent replicates for each experiment. (E) eDNA release of selected strains from three

1035 independent overnight cultures grown in CDM media. eDNA release was calculated by taking
1036 the arbitrary fluorescent units and dividing by the recorded OD₆₀₀ at the time of harvest. (F)
1037 Change in biofilm biomass compared to UA159 using CDM media with 15 mM glucose and 2.5
1038 mM sucrose as the carbohydrate source after 48 hours of growth. Each data point (n = 12 or n =
1039 8) represents an individual replicate. Statistical analysis was calculated by the Student's *t*-test; *
1040 P < 0.01.

1041
1042 *Figure 4. PcomX activities with addition of various synthetic XrpA peptides.* (A) Synthetic
1043 peptides synthesized for use in this study. The full-length, 69-aa XrpA protein is shown with
1044 each selected peptide highlighted by color and brackets. Below is a table with each peptide start
1045 and stop position in native XrpA, their sequences, and length in aa residues. Peptides S1 and
1046 S2, representing scrambled XrpA-1 and XrpA-2, were generated by the Shuffle Protein tool from
1047 www.bioinformatics.org with XrpA-1 and XrpA-2 serving as input sequences; S1 and S2 are of
1048 same length and aa composition as XrpA-1 and -2, respectively. (B) Transcriptional activation
1049 assays using *PcomX::gfp* reporter strain grown in CDM medium with addition of 10 μM of
1050 various synthesized XrpA peptides. (C) Direct comparison of transcriptional activation assays
1051 between XrpA-1 and a scrambled version of XpA-1. (D) Dose-dependent inhibition of *PcomX*
1052 activity by various concentrations of XrpA-1. Colored lines represent relative *PcomX* expression
1053 (arbitrary fluorescence units divided by OD₆₀₀, left axis). Black lines represent growth (OD₆₀₀,
1054 right axis) of each of the respective reporter strains during the assay. Each data point shown is
1055 the average of three independent biological replicates with four measured technical replicates.

1056
1057 *Figure 5. Addition of XrpA peptides changes lytic and competence phenotypes.* (A) eDNA
1058 release by UA159 in cultures to which 10 μM XrpA peptides were added. Results are from three
1059 independent overnight cultures grown in CDM media. eDNA release was calculated by taking

1060 the arbitrary fluorescence units and dividing by the recorded OD_{600} at the time of harvest. (B)
1061 Log_{10} fold change in transformation efficiency with 10 μM XrpA peptides compared to DMSO-
1062 only control (vehicle; set to 0) in FMC medium with 0.5 μM sXIP addition. Each data point
1063 represents a replicate ($N = 8$). (C) Western blot using 10 μg of whole cell lysates of UA159 with
1064 addition of 10 μM XrpA peptides in FMC medium with 0.5 μM sXIP addition. Cells were grown to
1065 $OD_{600} = 0.5$ before harvesting. Primary antisera, raised against the corresponding protein, were
1066 used for detection. ManL (the EIIAB domain of the glucose PTS permease) served as a loading
1067 control. All statistical analysis for this figure was calculated by the Student's *t*-test.

1068

1069 *Figure 6. Fluorescence Polarization confirms XrpA-ComR interactions.* Fluorescence
1070 polarization (FP) curves of increasing concentrations of purified ComR binding to 10 nM of
1071 *PcomX* dsDNA probe in the presence of 10 μM sXIP and 10 μM of various XrpA peptides
1072 (Figure 4A). Control (black lines) represent binding in the absence of XrpA peptides. (A) addition
1073 of XrpA peptides 1-4, (B) comparison between XrpA-1 and a scrambled version of XrpA-1, and
1074 (C) comparison between XrpA-2 and a scrambled version of XrpA-2. Data shown are averages
1075 from three independent experiments. K_d values are shown in Table 2.

1076

1077 *Figure 7. The N-terminus of XrpA inhibits ComR.* (A) Individual 2D gels of pIB184 (vector
1078 control; green) and ComR-Strep with 2 μM sXIP (red) elutions obtained during SPINE
1079 experiments, along with a merged image. The red arrows indicate regions where XrpA peptides
1080 were identified via spot picking and LC-MS/MS of trypsin-digested proteins. (B) Selection of
1081 XrpA-N1 and XrpA-N2 synthetic peptides based on the sequences returned by LC-MS/MS. The
1082 full length 69-aa XrpA protein is shown with each selected peptide highlighted by color and
1083 brackets. To the right is a table with the start and stop position of each peptide in XrpA, the
1084 peptide sequence, and the length in aa residues. (C) Transcriptional activation assays using a

1085 fused *PcomX::gfp* reporter strain in CDM medium with addition of 10 μ M of either XrpA-N1 or
1086 XrpA-N2 compared to DMSO control. (D) Fluorescence polarization (FP) curves of increasing
1087 concentrations of purified ComR binding to 10 nM of *PcomX* dsDNA probe in the presence of 10
1088 μ M sXIP and 10 μ M of either XrpA-N1 or XrpA-N2 compared to DMSO control. K_d values are
1089 shown in Table 2. Both transcriptional activation assay and FP assay results are averages from
1090 three independent experiments.

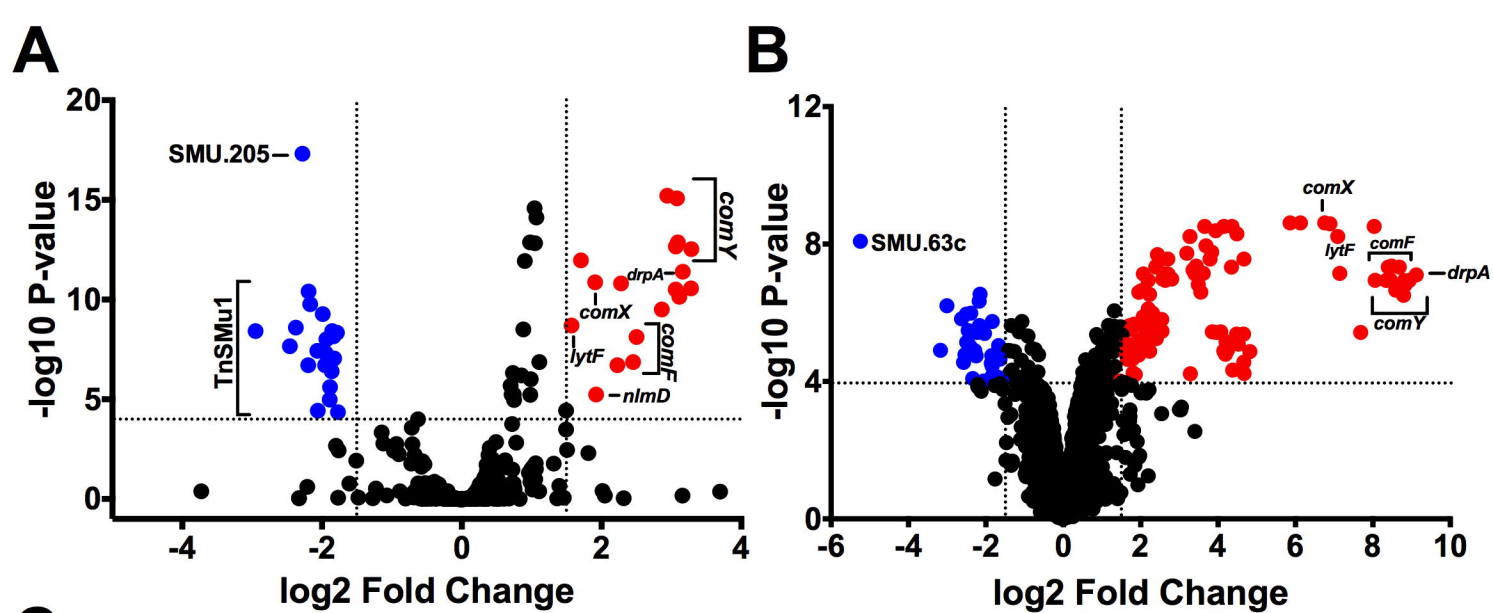
1091

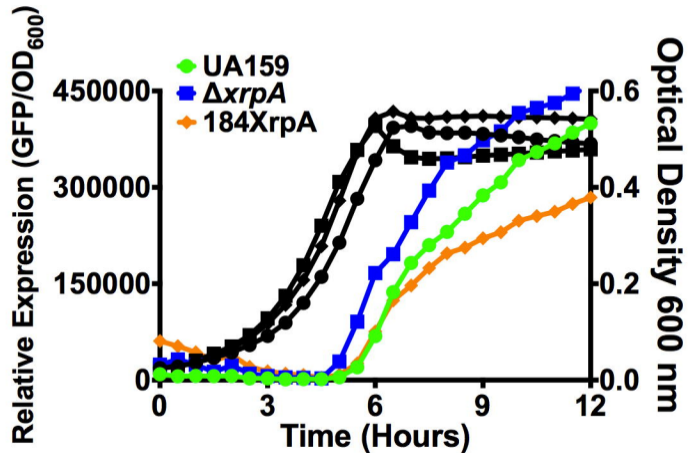
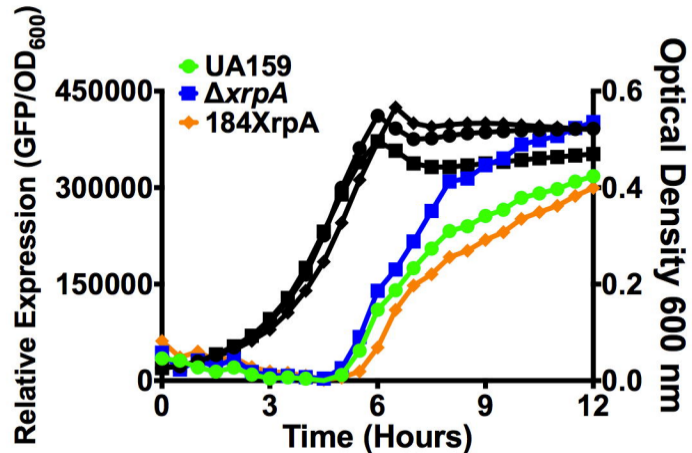
1092 *Figure 8. Fluorescence Polarization experiments with labeled XrpA-N1.* (A) Selectivity of FITC-
1093 labeled XrpA-N1 probe to ComR (black) over other *S. mutans* purified recombinant proteins
1094 SppA (blue) and CcpA (red). Fluorescent polarization (FP) curves were generated using
1095 increasing concentrations of purified proteins binding to 10 nM of fluorescently labeled XrpA-N1
1096 probe in the presence of 10 μ M sXIP. (B) Increasing concentrations of synthetic unlabeled
1097 XrpA-N1 peptide were assessed for their ability to compete with FITC-labeled XrpA-N1 for their
1098 binding to increasing concentrations of purified ComR. (C). Binding of 10 nM FITC-labeled
1099 XrpA-N1 peptide to increasing concentrations of purified ComR, with and without 10 μ M sXIP
1100 addition. (D) Binding of 10 nM FITC-labeled XrpA-N1 peptide to increasing concentrations of
1101 purified ComR in addition to increasing concentrations of sXIP peptide. Data shown for all
1102 graphs are averages of three independent experiments.

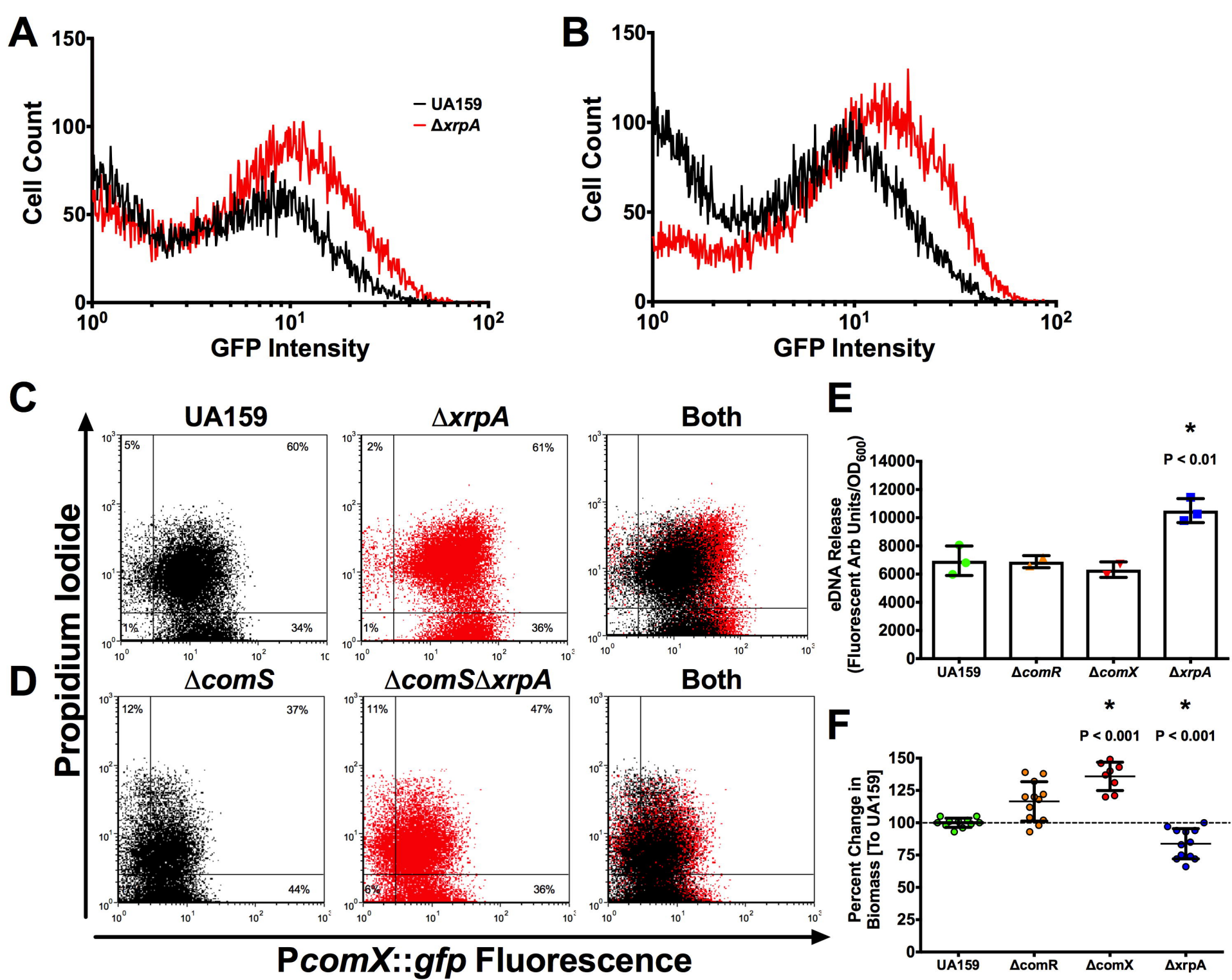
1103

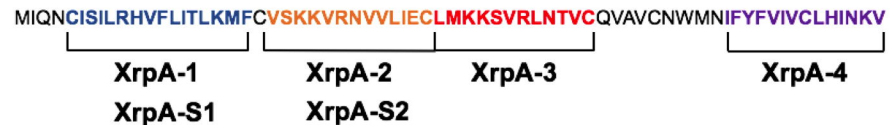
1104 *Figure 9. Model for XrpA Modulation of ComRS Signaling.* Current model for the role of XrpA in
1105 inhibition of ComRS activity and in cell fate. When present and active, XrpA (yellow) interacts
1106 with ComR (blue) independently of whether ComR is in a complex with XIP (orange), resulting
1107 in diminished affinity of ComR for its target in *PcomX*. XrpA inhibition of ComR prevents the
1108 ComR-XIP complex from over-amplifying the competence activation signal, thereby maintaining
1109 a balance within the population of cells that induce competence and internalize DNA with a

1110 group of cells that undergo lysis providing DNA as a nutrient source, a source for genetic
1111 diversification, and/or a source of eDNA that contributes to extracellular matrix formation. One
1112 potential mechanism by which XrpA curtails proficient ComR-XIP activation of *P_{comX}* is through
1113 inefficient dimer formation between ComR-XIP complexes. When XrpA is absent from the
1114 circuit, as in the case of the *xrpA* mutant ($\Delta xrpA$; *comX*::T162C), over-amplification of ComRS
1115 signaling occurs. This leads to increases in the accumulation of the sigma factor ComX (green);
1116 which in turn results in an increase in the subpopulation of cells that undergo cell lysis.
1117

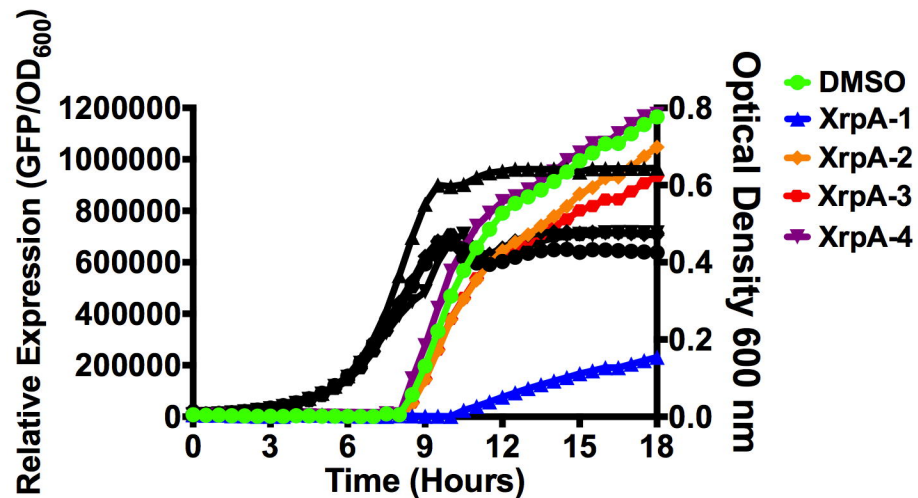
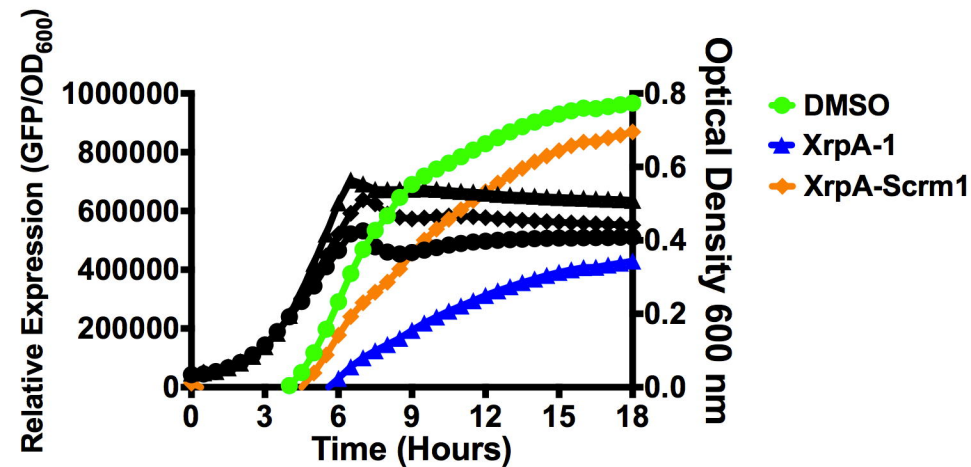
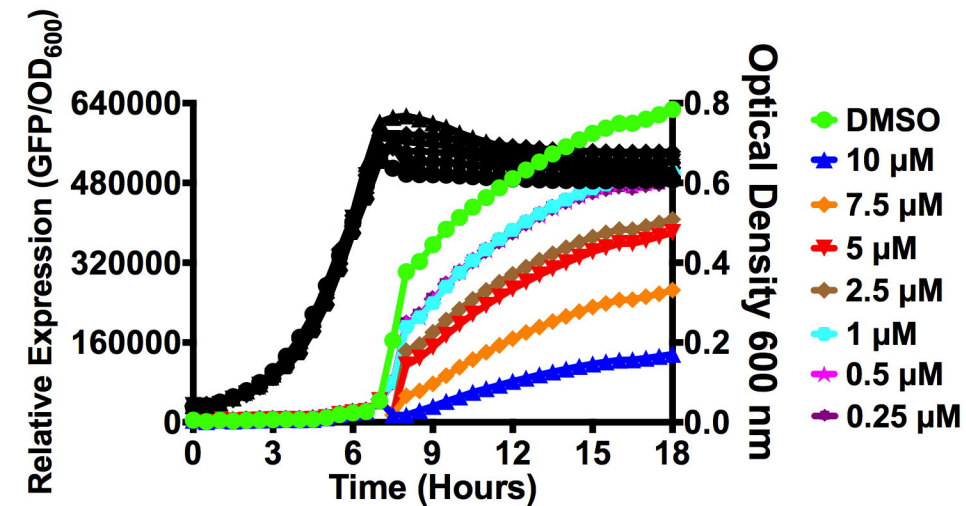


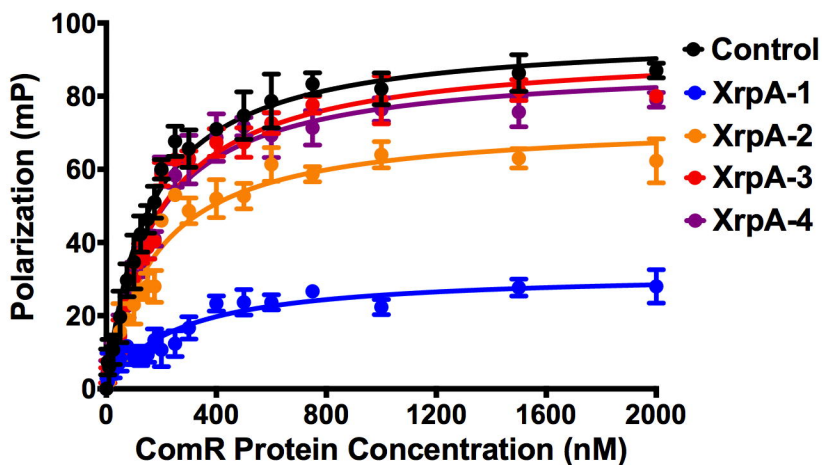
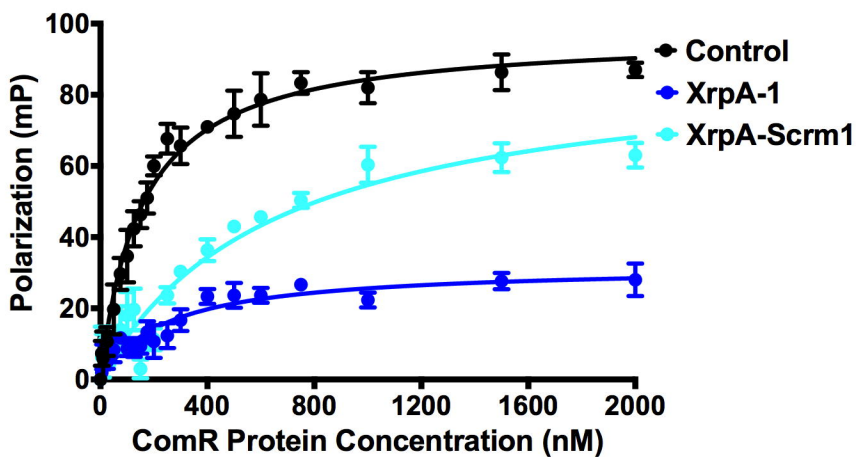
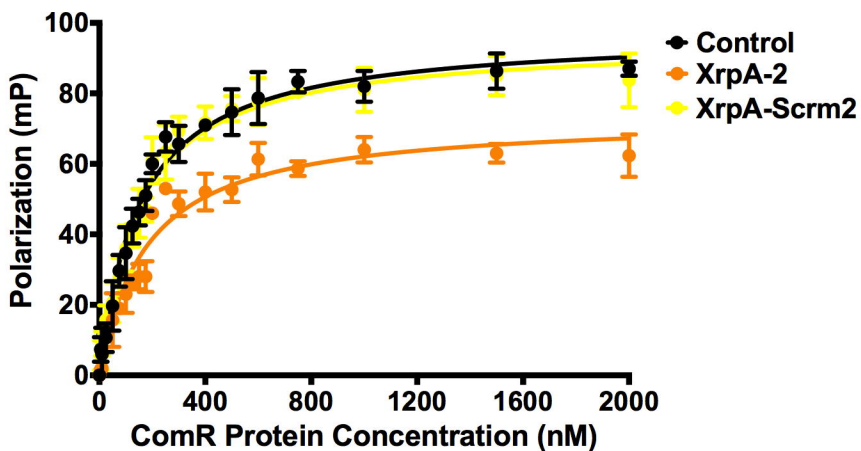
A**B**

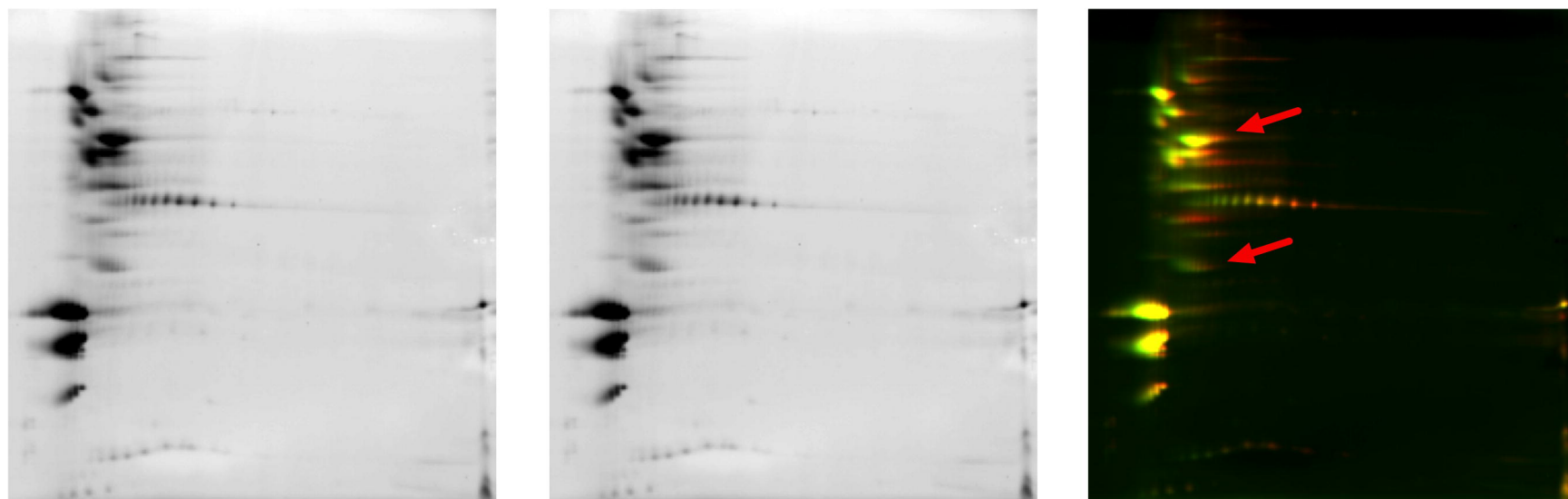


A

Peptide	Start Position	End Position	Sequence	Length
1	5	20	CISILRHVFLITLKMFC	16
2	22	34	VSKKVRNVVLIIEC	13
3	35	46	LMKKSRLNTVC	12
4	56	69	IFYFVIVCLHINKV	14
S1			LFKFTCVRLILIIISHM	16
S2			KKNVIECVSVRVL	13

B**C****D**

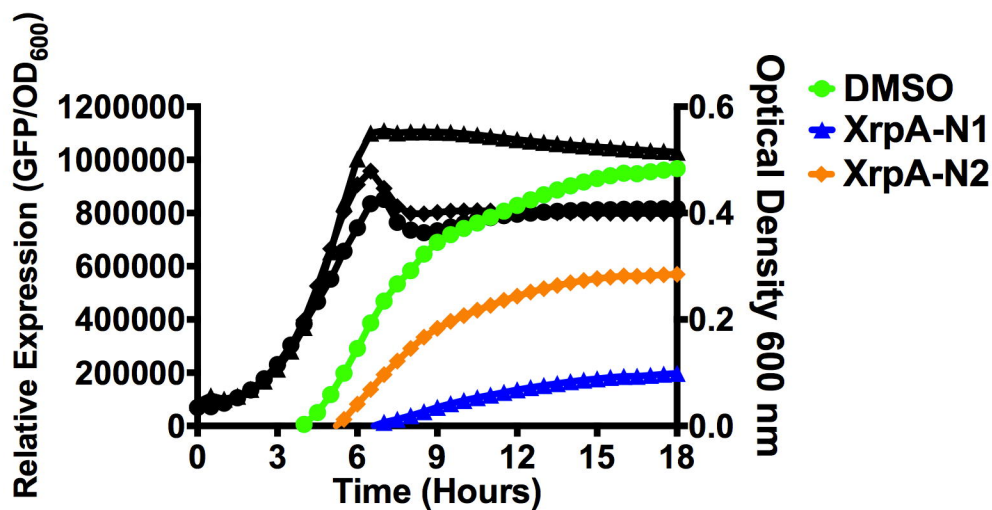
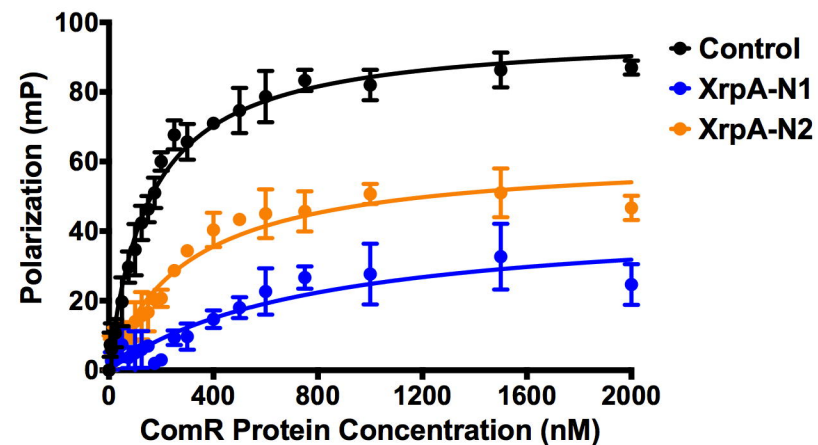
A**B****C**

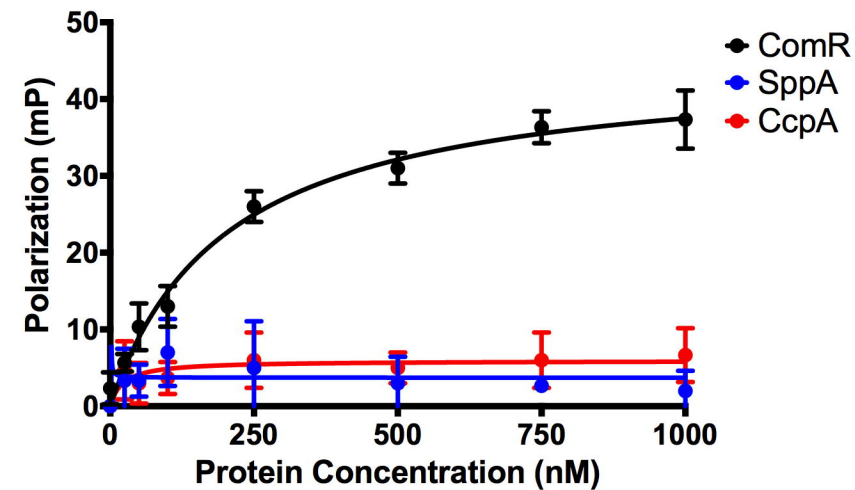
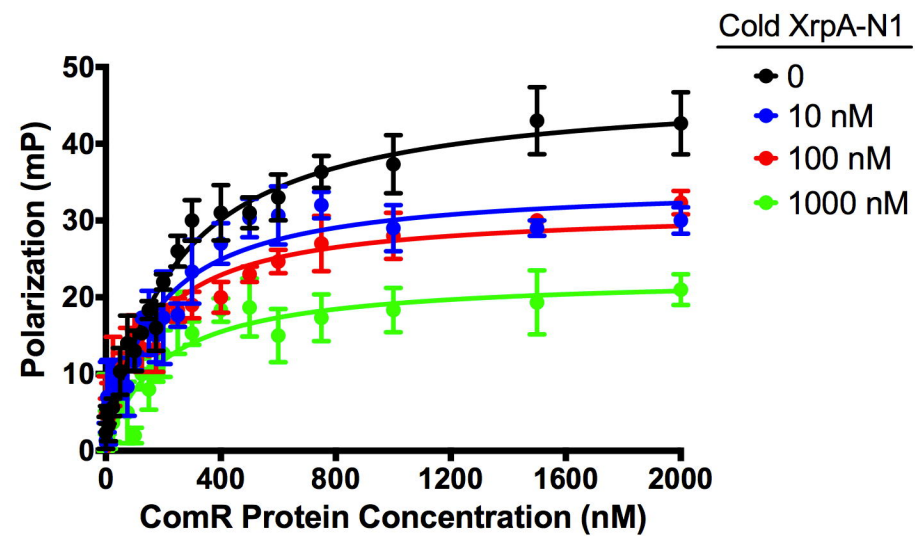
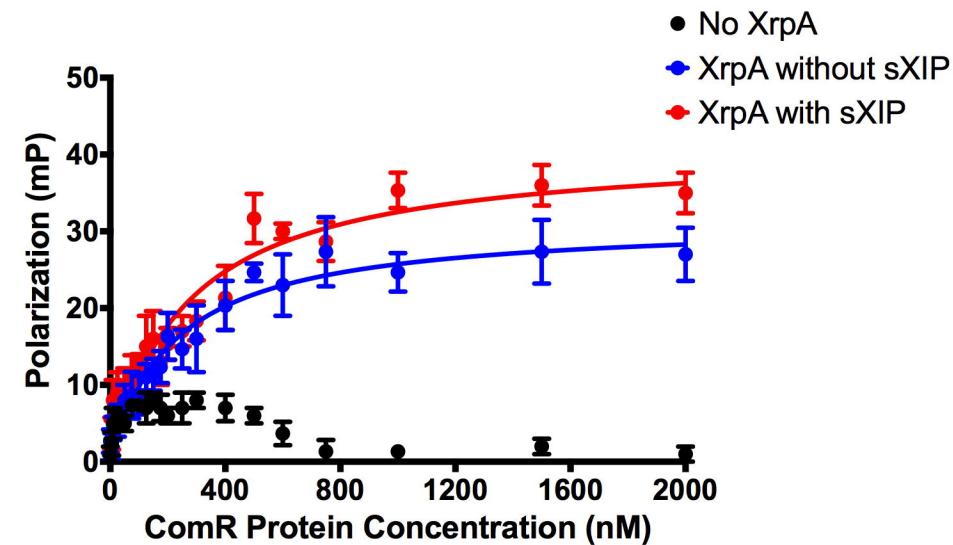
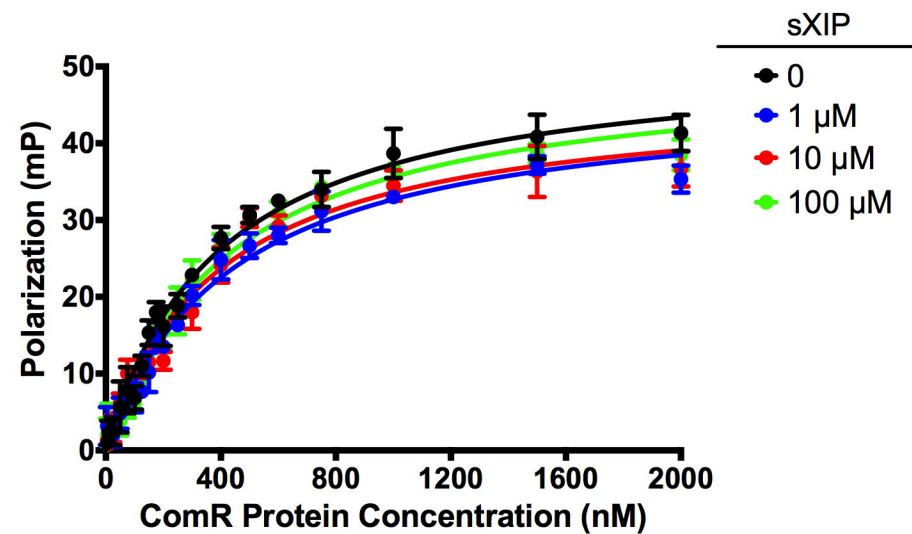
A**pIB184 (Vector Control)****ComR-Strep (+ XIP)****Merged****B**

MIQNCISILRHVFLITLK**MFCVSKKVRNVV**LIECLMKKSVRLNNTVCQVAVCNWMMNIFYFVIVCLHINKV

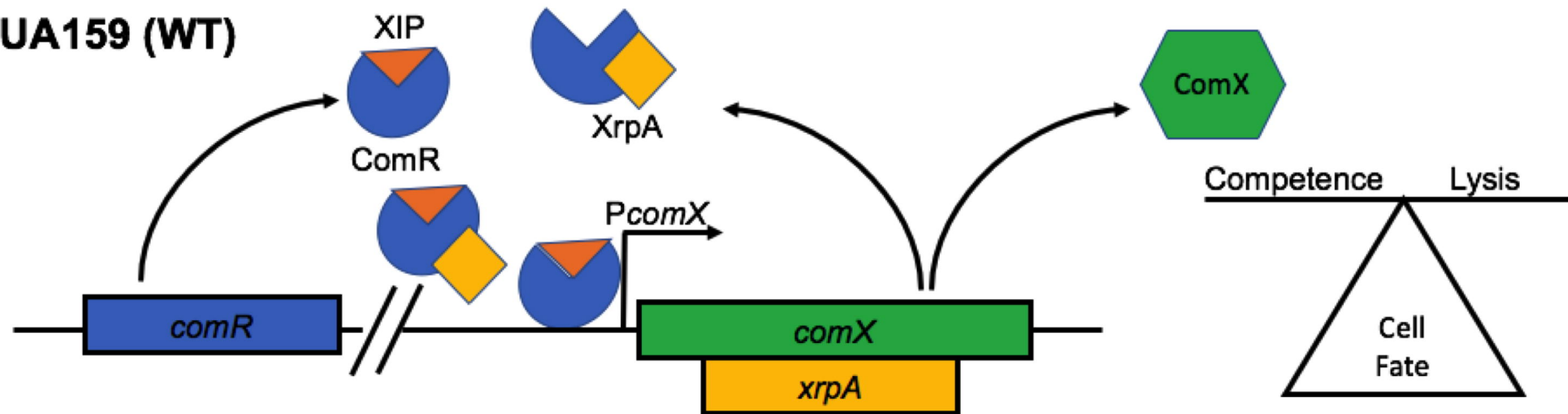
XrpA-N1 XrpA-N2

Peptide	Start Position	End Position	Sequence	Length
N1	1	18	MIQNCISILRHVFLITLK	18
N2	18	38	MFCVSKKVRNVV LIECLMKK	20

C**D**

A**B****C****D**

UA159 (WT)



$\Delta xrpA$ (*comX*::T162C)

